KAPL-P-000143
(K97003)
CONF-970824--

CRITICAL HEAT FLUX EXPERIMENTS IN A HEATED ROD BUNDLE WITH UPWARD CROSSFLOW OF FREON 114

P. D. Symolon, W. E. Moore, D. F. Wolf

February 1997

NOTICE

KAPL ATOMIC POWER LABORATORY SCHENECTADY, NEW YORK 10701

Operated for the U. S. Department of Energy
by KAPL, Inc. a Lockheed Martin company

DISCLAIMER

Critical Heat Flux Experiments in a Heated Rod Bundle with Upward Crossflow of Freon 114

PD Symolon WE Moore and DF Wolf

Abstract

Critical heat flux (CHF) data were obtained for upward crossflow of R-114 in a heated staggered rod bundle. Data were obtained over a broad range of mass fluxes (135 to 1,221 kg/m^{2}sec), inlet subcooling (0 to 55^{o}C), and qualities (-0.42 to 0.92). The present work extends the available database to higher quality, inlet subcooling, and mass flux. The test section is 3.43 cm x 15.24 cm (1.35in. x 6in.) in cross section with a total length of 55.88 cm (22") from the top of the inlet flow straightener to the perforated plate at the test section exit. The rod bundle has a triangular pitch with a diameter (D) of 0.635 cm (0.25 in), and a pitch to diameter (P/D) ratio of 1.5. The rod bundle has 165 rods with a 15.24 cm (6 in.) heated length arranged in 55 rows of three rods each. Unheated half rods were positioned on the walls of the test section to maintain the regular rod arrangement and prevent flow bypass along the gaps between the window and the first column of heated rods. A single instrumented heater was positioned five rows upstream from the bundle exit to determine CHF. The last three rows of rods in the bundle were unheated to prevent undetected dryout downstream of the CHF position. Temperature excursions due to CHF were sensed using four imbedded thermocouples (TC) in the heater rod. The four TC temperatures were continuously monitored on a strip chart recorder. The rod heat was gradually increased until CHF was detected. Overall, the data are in good agreement with the Jensen and Tang correlation in the range of application of this correlation. The local minima in CHF which occurs near zero quality is slightly lower in the present experiment than for the Jensen and Tang correlation. At high quality, CHF drops off more rapidly than the Jensen-Tang prediction. Data are now available to extend the existing correlations to higher quality, and higher inlet subcooling.

1.0 Introduction

CHF in multi-rod bundles has been investigated experimentally by Leroux and Jensen (1992) and Dykas and Jensen (1992). These data were used to develop the correlation of Jensen and Tang (1994). CHF correlations were also developed by Yao and Huang (1989) for a multi-rod bundle and Katto et al. (1987) for a single rod with subcooled flow. Table 1 compares the range of conditions of the present test with those of other investigators. The data of Yao and Huang is limited to low quality, and Katto obtained data for subcooled conditions only. The present work extends the available database to higher quality, higher inlet subcooling, and higher mass flux.

2.0 Test Description

A schematic of the test section inlet heater system is provided in Figure 1. The inlet heaters were used to increase the temperature of the Freon, and the trim heaters and/or test section heaters were used to bring the Freon up to the desired quality at the elevation of the CHF rod. A schematic of the test section is provided in Figure 2. A vertical tube support plate oriented perpendicular to the heater rods was installed at the test section midplane, dividing the test section flow into two parallel paths, which merged in the upper plenum. The CHF measurements were performed

in the flow path at the right side of the test section. The un-instrumented heater rods were heated for the full 6 inch test section width. The CHF rod was heated over the 2.75 inch rod length that was in the flow path on the right. This was done to prevent CHF from occurring in the un-instrumented left side of the test section.

Four thermocouples were installed on the heater rod, three on the top side of the rod, and one on the under side near the center of the heated length of the rod (Figure 2). The thermocouples are 20 mil sheathed grounded junction type T thermocouples which were embedded in grooves in the surface of the heater rod using soft solder. The four TC temperatures were continuously monitored on a strip chart recorder. The recorder speed was 2mm/sec and the temperature range was 140°F to 190°F (60°C to 87°C) for a 40mm span. Temperature fluctuations as small as ±1°F (±.55°C) and as brief as 0.1 sec were easily observed. A 5% higher heat flux was established for 0.5 inches at the location of the TCs by increasing the density of the resistance winding in the heaters Thus the local heat flux at the CHF location can be calculated from:

$$q'' = 1.05\frac{P_{rod}}{\pi D L_h}$$

Where P_{rod} is the rod CHF power, D is the rod diameter, and L_h is the heated length of the rod.

3.0 Test Data

The CHF test results are provided in Table 2, which tabulates the following parameters:

- Bundle averaged quality (from energy balance) at axial position of CHF rods
- Test section mass flux (kg/m^2-sec) at the location of the rod gaps (minimum flow area)
- Power to test section (non-CHF) heater rods (kW)
- Test section heat flux (kW/m^2) for the non-CHF heater rods
- Critical heat flux, CHF, (kW/m^2)
- Run number
- Type of CHF (temperature excursion, or change in slope of temperature vs. power plot)

The test matrix includes five different mass flow rates, with a range of qualities tested for each flow rate. All of the data were obtained at a pressure of 90 psia. For cases with positive quality at the CHF location (x>0), the test section inlet temperature was set to a few degrees below the saturation temperature, and power was applied to the test section heaters to achieve the desired quality. If the test section heaters were at maximum power (30kW) and the desired quality was not achieved, then the inlet trim heaters were used to increase the quality by providing boiling two phase flow to the inlet of the test section. For the subcooled or negative quality (x<0) cases, all of the rods in the bundle were unheated except for the instrumented CHF heater rod.

An energy balance corrected for heat losses was used to determine the quality. The magnitude of the test section heat loss was determined to be approximately 100 watts based on single phase heat loss runs. The quality, x, was calculated from the measured inlet temperature, flow rate and power input, and system pressure from a heat balance:

$$x = \frac{P_{in} - Q}{w h_{fg}} - \frac{C_p (T_{sat} - T_{in})}{h_{fg}}$$

Where P_{in} is the power input, Q is the heat loss, w is the mass flow rate and T_{in} is the inlet temperature. T_{sat} is the saturation temperature at the measures system pressure, C_p is the heat capacity and h_{fg} is the enthalpy of vaporization.

The CHF data were obtained by first setting up the test conditions with CHF rods operating at about the same power as the non-CHF rods. The power to the CHF rod was increased in small (~10 to 25 watt) increments, while observing the strip chart for the onset of CHF. If a temperature excursion did not occur after the onset of CHF, smaller (~5 watt) power increments were used to better define the change in slope. The TC#1 temperature was plotted as a function of power. Typical strip chart results, and average temperature versus power graphs are provided in Appendix A. The strip charts show the four thermocouples, the test section pressure, and the CHF heater power.

Two distinct types of CHF were observed. For subcooled conditions, the onset of CHF was observed to be a sudden excursion of the wall temperatures (See Figures A.4 to A.9). This excursion came without warning or any significant temperature fluctuations. For the lowest flow runs with inlet subcooling (Runs 174 and 179 at G=135 kg/m^{2}sec), a slight change in slope was observed prior to the temperature excursion (Figures A.4 and A.9). Failure of the instrumented heaters was prevented by automatic over-temperature power cutout circuitry. The power cut-off can be seen in the strip chart recordings. For bulk quality conditions, the onset of CHF resulted in a change in slope of the temperature versus power plot, and the intersection of the two different slopes defined the CHF condition. This change in slope was quite small for some conditions (Figure A.1) but for other conditions was dramatic (Figure A.3).

For bulk boiling conditions, the TC strip chart recordings exhibited random temperature fluctuations due to surface boiling which increase as the rod power was increased. This resulted in frequent 3 to 6^{o}C (5 to 10^{o}F) spikes near the CHF power setting. As power was further increased, simultaneous spikes were observed on all three thermocouples on the upper side of the heated rod, but the TC on the lower side remained relatively quiet. This behavior is thought to represent the formation of a small vapor patch on the top surface of the rod which is quickly swept away by the flow. An example is shown in Figure A.10. Usually the bottom TC was very quiet; however for high quality runs correlated temperature fluctuations were observed on all four thermocouples, as shown in Figures A.1, A.2 and A.3. Apparently, these events represent vapor patches forming entirely around the heater rod.

For one of the runs (Figure A.2) a decrease in the slope of the temperature versus power plot was observed with increasing power. The reason for this behavior may have been an improvement in surface heat transfer due to thin film evaporation, which sometimes occurs just prior to CHF (Lahey and Moody, 1977). However, the strip chart recording did indicate 8-10 ^{o}F temperature spikes, so the point was included as CHF data.

The experimental error in the CHF measurement was estimated to be about ±3% of the CHF power. Several repeat runs were made, and the results were within the experimental uncertainty. For several test runs, the temperatures at the top of the rod were also plotted for decreasing power to investigate hysteresis effects associated with re-wetting the CHF surface. No hysteresis effects were observed. For the same local quality at the CHF position (19%) a comparison was made for G=678 kg/m^{2}sec with and without heat applied to the test section heaters . This pair of runs (996 and 1010 in Table 2) was made to determine if heat flux on the rods neighboring the CHF rod had any influence on CHF power. It was found that if the heat is applied to the neighboring rods, the CHF is approximately the same as for adiabatic rods with quality introduced at the test section inlet.

Leroux and Jensen (1992) defined the CHF condition as the point of a distinct but small rise in the slope of the resistance of the CHF rod caused by the formation of a stable film boiling patch. Figures 3 and 4 compare the present CHF data (P/D=1.5) with data of Leroux and Jensen (P/D=1.3) obtained at similar test conditions. The low flow data (G~100 kg/m^{2}sec) in Figure 3 for both bundles exhibits a continuously decreasing CHF with increasing quality. For the higher flow (G~400 kg/m^{2}sec) in Figure 4 CHF decreases to a local minimum (which occurs near zero quality), increases to a local maximum, then decreases.

4.0 Comparison of Test Data with Correlations

4.1 CHF Correlations for Crossflow Rod Arrays

The test results were compared to the correlations of Jensen and Tang (1994), Yao and Huang (1989) and Katto et al (1987). The Katto correlation is for CHF on a single tube in crossflow of a subcooled liquid, while Jensen and Tang, and Yao and Huang correlations are for multi-rod bundle at net quality conditions with only the CHF rod heated. For the present test, the entire bundle of rods were heated at a heat flux well below CHF to vary the local quality, and the power applied to the instrumented CHF heater was increased to the CHF condition.

Jensen and Tang (1994) developed correlations for CHF on a single heated tube in a staggered or in-line bundle using R-113. Unlike the present test, only the CHF rod was heated. In developing their correlation, the CHF data were divided into three distinct regions: a low quality departure from nucleate boiling region (Region I), a high quality film dryout region (Region III) and an intermediate transition region (Region II). For a staggered bundle with a pitch to diameter ratio of 1.3, the correlations for Regions I and III can be written as:

$$\text{Region I:}\quad q''_{CHF} = q''_{max}\exp\left(-0.0322 - \frac{10.1}{\psi^{0.585}}\right)$$

$$\text{Region III:}\quad Bo = \frac{q''_{CHF}}{Gh_{fg}} = 1.97\cdot 10^{-2}A^{0.165}Re^{-0.0858}$$

where:

$$q''_{max} = K\rho_v^{1/2}h_{fg}(\sigma g\Delta\rho)^{1/4}$$

$$A = \frac{g\rho_{tp}\Delta\rho D}{G^2}$$

$$\rho_{tp} = \left(\frac{1}{\rho_l} + x\left(\frac{1}{\rho_v} - \frac{1}{\rho_l}\right)\right)^{-1}$$

$$K = 0.1164 + 0.297\exp(-3.44\sqrt{R_\sigma})$$

$$R_\sigma = \frac{D}{2}\left(\frac{g\Delta\rho}{\sigma}\right)^{1/2}$$

$$\psi = \frac{\rho_{tp}}{\mu_l} D\left(\frac{\sigma g\Delta\rho}{\rho_l^2}\right)^{1/4}$$

$$Re = \frac{GD}{\mu_l}$$

Region II is calculated as a linear interpolation between Regions I and III where the transition between the regions occurs at:

$$x_{I-II} = 0.242A^{0.396}$$

$$x_{II-III} = 0.432A^{0.098}$$

Katto et al (1987) developed a CHF correlation for a single 1mm diameter cylinder in crossflow of a subcooled liquid:

$$\frac{q''_{CHF}}{Gh_{fg}} = \left[0.00588 + 0.5\left(\frac{\rho_v}{\rho_l}\right)^{1.11}\right]\left(\frac{\sigma\rho_l}{G^2D}\right)^{0.42\left(\frac{\rho_v}{\rho_l}\right)^{0.0428}}$$

Yao and Huang (1989) developed the following correlation based on their data:

$$\frac{q''_{CHF}}{Gh_{fg}} = \frac{\rho_v}{\rho_l}(0.594(We)^{-0.476}(1-x)^{0.954})(R_\sigma^{0.36})\left(2.25 + \left(\frac{\rho_v}{\rho_l}\right)^{0.15}\right)^{-1}\left(1 - \left(\frac{D}{2P}\right)^{0.86}\right)$$

Where R_σ is as defined above, and the weber number is:

$$We = \frac{\rho_g DG^2}{\sigma\rho_l}$$

The Jensen and Tang, Yao and Huang (for $x>0$) and Katto et al. (for $x<0$) CHF correlations are plotted in Figure 5 for three values of the mass flux. The Katto et al. correlation, which is for a single tube, gives a lower value of CHF than does the Jensen and Tang correlation at zero quality. The CHF of the Jensen-Tang correlation increases with mass flux. The Kato et al correlation does not include a subcooling effect, which data from this study indicates is necessary. The Yao and Huang correlation predicts a decreasing CHF with increasing quality. At high mass flux, Jensen-Tang predicts a decreasing CHF with quality, followed by a rapid increase to a maximum value, then a gradual decrease with increasing quality.

4.2 Comparison of Test Data with CHF Correlations

The Jensen and Tang staggered rod CHF correlation was based on test data for a P/D=1.3, while the present data is for a P/D=1.5 so, some differences between the data and the correlation are expected. Comparisons of the CHF data with the Jensen and Tang correlation are provided in Figures 6, 7, and 8 for G=135, 407, and 678 kg/m^2-sec respectively. Figures 9 and 10 provide the comparisons for the two high flow data sets (G=950 and 1221 kg/m^2-sec, respectively). The correlation is plotted over a quality range of zero to 70%, which encompasses the range of data originally used to develop the correlation. For the two high flow runs the available test section and trim heater power limited the maximum quality to about 15%, so it was not possible to determine the local maximum in CHF, which is predicted to occur at about 30% quality. The local minimum was lower than the correlation, but the data confirmed the predicted trend of a sharply increasing CHF with increasing quality. This minimum in CHF near zero quality was also observed by Inoue and Lee (1996) for a vertical rod in an annulus. At low flow (G=135 kg/m^2-sec) in Figure 6, the decreasing CHF data with increasing quality is in agreement with the correlation of Jensen and Tang. However, at high quality, the CHF data decreases more rapidly than the prediction. In the transitional regime where CHF increases with quality (Region II), the present data is in fairly good agreement with the correlation. This is exhibited in Figures 7, 8, 9, and 10. However in Region III where CHF is decreasing with increasing quality, the P/D=1.5 CHF data begins to decrease more rapidly with quality at a lower quality than the Jensen-Tang correlation (see in Figures 7 and 8). This suggests that at higher quality conditions, the CHF performance of a staggered bundle with P/D=1.5 is lower than for P/D=1.3.

For G=135, 678 and 1221 kg/m^2-sec (Figures 6, 8, and 10, respectively) data points were also taken for subcooled conditions. These three data sets and the correlation are plotted in Figure 11. The subcooled data indicates increasing CHF for increasing mass flux, and increasing subcooling. In this plot the Jensen-Tang correlation was extrapolated to subcooled conditions by simply applying the Region I correlation for negative qualities, using the liquid density in place of the two phase density. The correlation has approximately the correct trend with quality (or subcooling) but has no mass flux dependence.

5.0 Conclusions

Overall, the Jensen and Tang correlation was found to predict the trends in the present data fairly well in the range of application of this correlation. The local minima in CHF which occurs near zero quality is slightly lower in the present experiment than for the Jensen and Tang correlation. Additionally, for high quality the present CHF data decreases earlier and more rapidly with quality than the correlation. This may be due to the higher P/D ratio (1.5 in the present test versus 1.3 for the Dykas and Jensen data). It is reasonable that CHF would be lower for higher P/D, since the size of the recirculation zone on the downstream side of the tubes would tend to be reduced in size for a more tightly packed pin bundle, reducing vapor accumulation and providing a more uniform distribution of film thickness on the rod. Data are now available to extend the existing correlations to higher quality, and higher inlet subcooling.

References:

Jensen, M.K. and Tang, H. "Correlations for the CHF condition in Two-Phase Crossflow Through Multitube Bundles" , Journal of Heat Transfer, Vol 116, August 1994.

Katto, Y., Yokoya, S., Miake, S., and Taniguchi, M. "Critical Heat Flux on a Uniformly Heated Cylinder in a Cross Flow of Saturated Liquid over a Wide Range of Vapor-to-Liquid Density Ratio" Int. J. of Heat and Mass Transfer, Vol. 30., No. 9, pp 1971-1977 (1987).

Leroux, K.M. and Jensen, M. K. "Critical Heat Flux in Horizontal Tube Bundles in Vertical Crossflow of R113", ASME Journal of Heat Transfer, Vol. 114 pp. 179-184, 1992.

Yao, S.C. and Huang, T.H. "Critical Heat Flux on Horizontal Tubes in an Upward Crossflow of Freon-113, "International Journal of Heat and Mass Transfer", Volume 32, pp. 95-103, 1989.

Dykas, S., and Jensen, M.K., "Critical Heat Flux on a Tube in a Horizontal Tube Bundle," Experimental Thermal and Fluid Science", Vol5, pp. 34-39, 1992.

Inoue, A. and S. Lee, "Influence of Two-Phase Flow Characteristics on CHF at Low Pressure", International Conference on Nuclear Energy" (ICONE-4), New Orleans Lousiana, March 1996.

R.T. Lahey and F.J. Moodey, Thermal Hydraulics of a Boiling Water Nuclear Reactor, ANS, 1977.

Nomenclature

Bo	Boiling number
D	Rod diameter
ρ_l	Density of the liquid phase
ρ_v	Density of the vapor phase
C_p	Heat capacity
T_{ex}	Exit temperature
T_{in}	Inlet temperature
T_{sat}	Saturation temperature
T_{sub}	Inlet subcooling = T_{sat}-T_{in}
P_{in}	Power input from non-CHF heaters
P_{rod}	Power input from CHF heater
P	Pitch (distance between rod centers)
q''_{CHF}	Critical Heat Flux
Q	Heat loss from test section or trim heaters
Re	Reynolds Number
h_g	Vapor enthalpy
h_f	Enthalpy of saturated liquid
h_{fg}	Enthalpy of vaporization
G	Average mass flux
w	Mass flow rate through test section
q"	Heat flux
X	Flowing quality
α	Void fraction
σ	Surface tension
μ_l	Viscosity of liquid phase
$\Delta\rho$	Change in density (ρ_l-ρ_g)

Table 1: Crossflow CHF Data in Multi-rod Bundles

Investigator and Test Configuration	Fluid	Test Section	Quality	Pressure (bar)	Mass Flux (Kg/m^2-sec)	Subcooling (Deg C)
Present work staggered triangular array	R-114	P/D=1.5 D=6.1mm	-0.42 to 0.92	6.1 bar	135 to 1221	0 to 55
Yao and Huang (1989) in-line square array	R-113	P/D=1.5 D=19.1mm	0 to 0.14	1 bar	132 to 560	0 to 6
Leroux and Jensen (1992) in-line square array and staggered triangular array	R-113	P/D=1.7 P/D=1.3 D=7.94mm	0 to 0.70	1.5 to 5 bar	50 to 500	0
Dykas and Jensen (1992) in-line square array	R-113	P/D=1.3 D=7.94mm	0 to 0.70	1.5 to 5 bar	50 to 500	0

Table 2: CHF data

Quality	Mass Flux (kg/m^2sec)	TS Power[(1)] (kW)	TS Heat Flux (kW/m^2)	CHF (kW/m^2)	Run No.	Type of CHF
-0.42	135	0.0	0	326	174	excursion
-0.24	135	0.0	0	301	179	Δslope, then excursion
0.06	135	1.17	2.4	232	982	Δslope
0.18	135	3.53	7.3	209	981	Δslope
0.25	135	5.89	12	215	980	Δslope
0.36 0.36 0.35	135	8.26	17	198 191 -	983 986 170	Δslope Δslope non-CHF
0.46	135	10.63	22	171	984	Δslope
0.56	135	12.99	27	154	985	Δslope
0.73	135	17.6	37	92	171	Δslope
0.81	135	20.0	42	68	172	Δslope
0.92	135	22.5	47	30	173	Δslope
0.036	407	2.53	5.3	198	993	Δslope
0.086	407	6.08	12	188	994	Δslope
0.14	407	9.63	20	215	995	Δslope
0.24	407	16.7	35	245	1003	Δslope
0.34	407	23.8	49	268	1004	Δslope
0.43	407	30	63	264	1005	Δslope
0.58	407	30	63	185	180	Δslope
0.73	407	30	63	130	181	Δslope
0.75	407	30	63	83	182	Δslope

Quality	Mass Flux (kg/m^2sec)	TS Power[1] (kW)	TS Heat Flux (kW/m^2)	CHF (kW/m^2)	Run No.	Type of CHF
-0.42	678	0.0	0	386	175	excursion
-0.24	678	0.0	0	311 317	1000 178	Δslope Δslope then excur.
0.028	678	3.89	8.1	192	987	Δslope
0.082	678	9.81	20	218	1009	Δslope
0.13	678	15.73	33	247	988	Δslope
0.187 0.190[2]	678	21.64 0.0	45 0	277 273[2]	1010 996	Δslope Δslope
0.23	678	27.55	57	305	989	Δslope
0.30	678	30	63	262	1001	Δslope
0.44	678	30	63	245	1002	Δslope
0.004	950	5.26	11	177	1008	Δslope
0.086	950	13.54	28	243	1007	Δslope
0.14	950	21.82	45	275	1006	Δslope
-0.42	1221	0.0	0	490	176	excursion
-0.24	1221	0.0	0	414	177	excursion
0.03	1221	6.63	14	181	992	Δslope
0.08	1221	17.27	36	260 270	991 998	Δslope
0.13	1221	27.92	58	328	990	Δslope

(1) -The test section power was limited to 30kW by the power supply. If the total power exceeds 30 kW, the remaining power in provided by the trim heaters.

(2)- Run 996 was obtained at same quality as run 1010, but with the test section adiabatic (Quality was introduced at the inlet using trim heaters)

Figure 1
Schematic of Test Section and Inlet Heater System

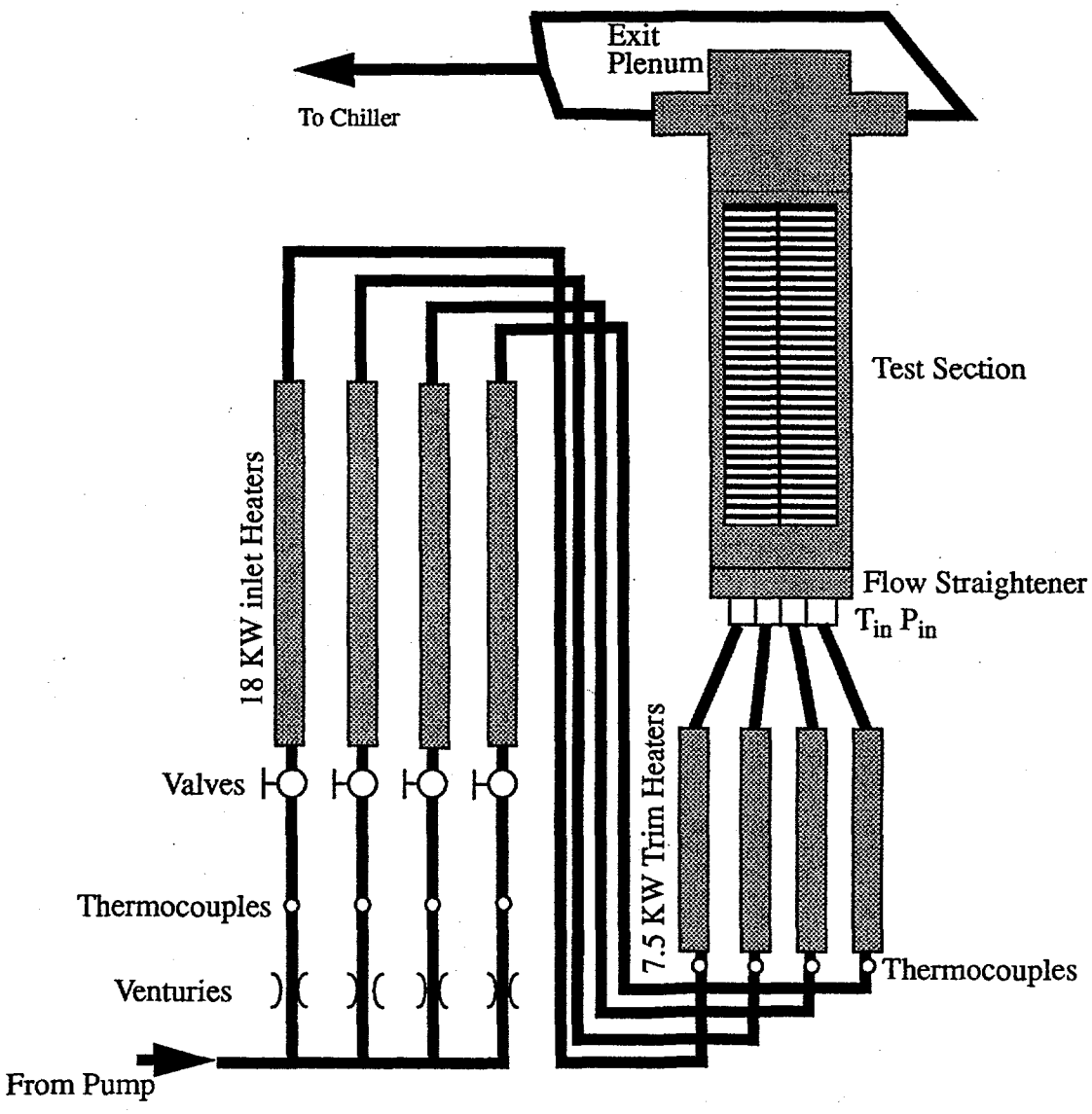

Figure 2
Test Section Rod Arrangement

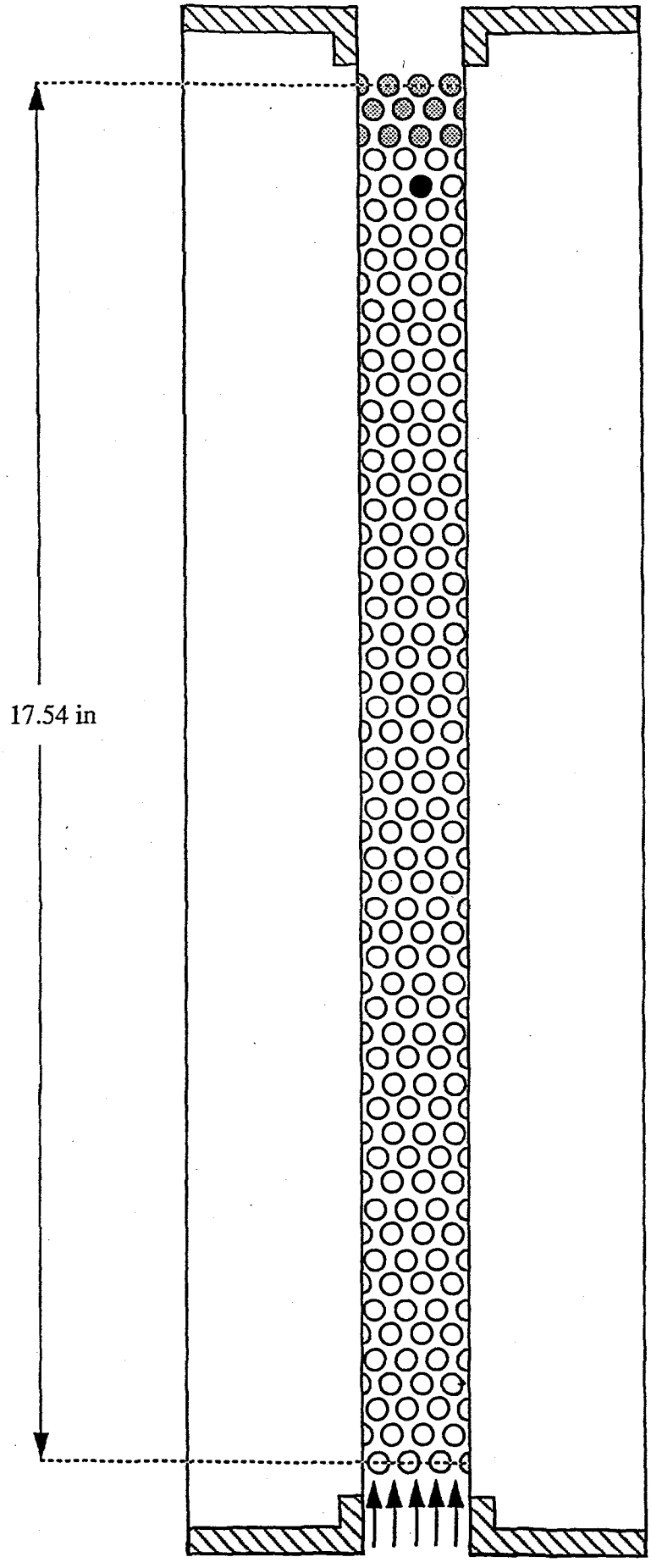

○ Heated rod

⊗ Unheated rod

● Instrumented heated rod

D Unheated half-rod

TC Arrangement on Instrumented Rod

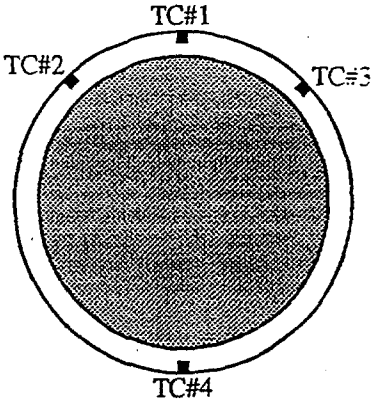

Figure 3: CHF Data Comparison for G~100 kg/m^{2}sec

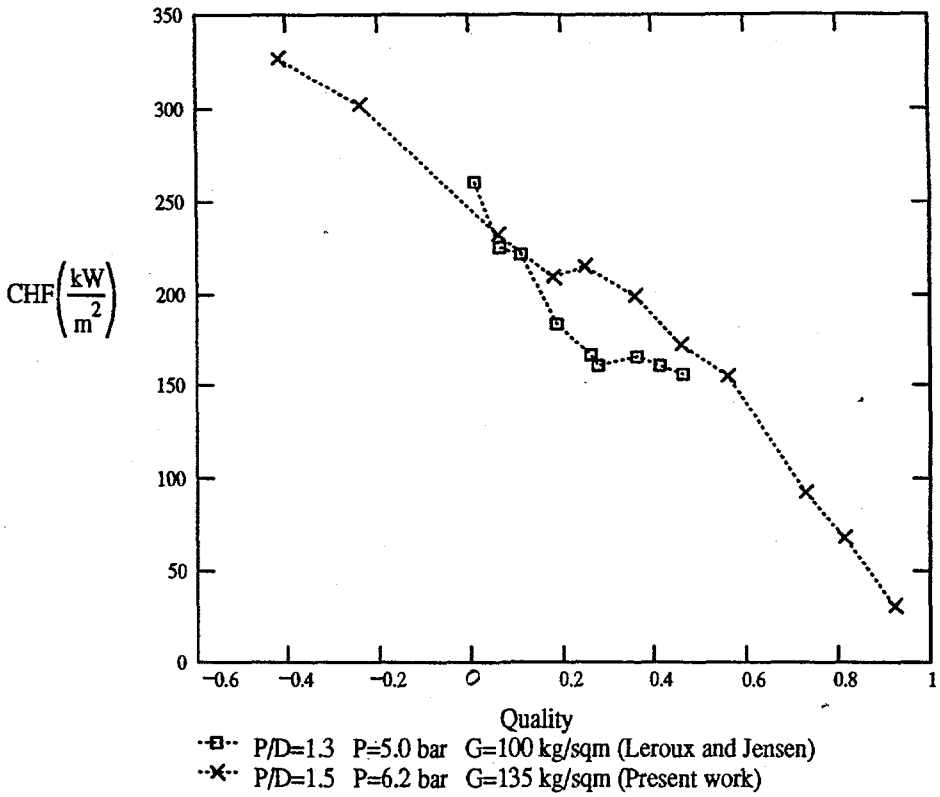

Figure 4: CHF Data Comparison for G~400 kg/m^{2}sec

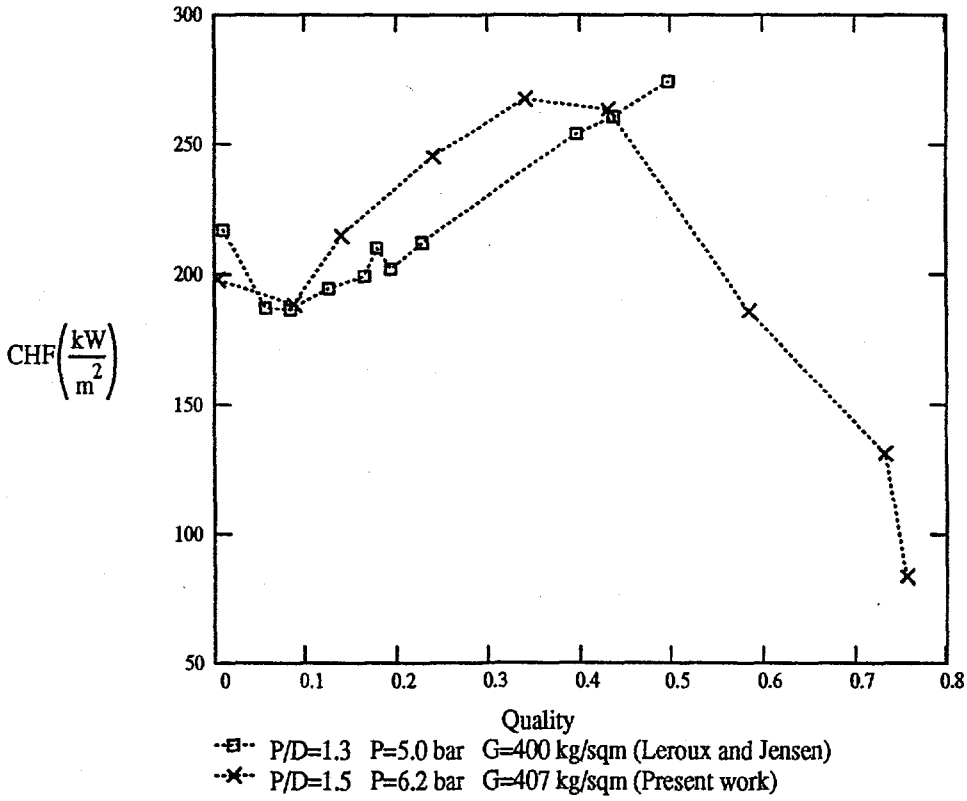

Figure 5
CHF Correlations for Subcooled and Saturated Regions

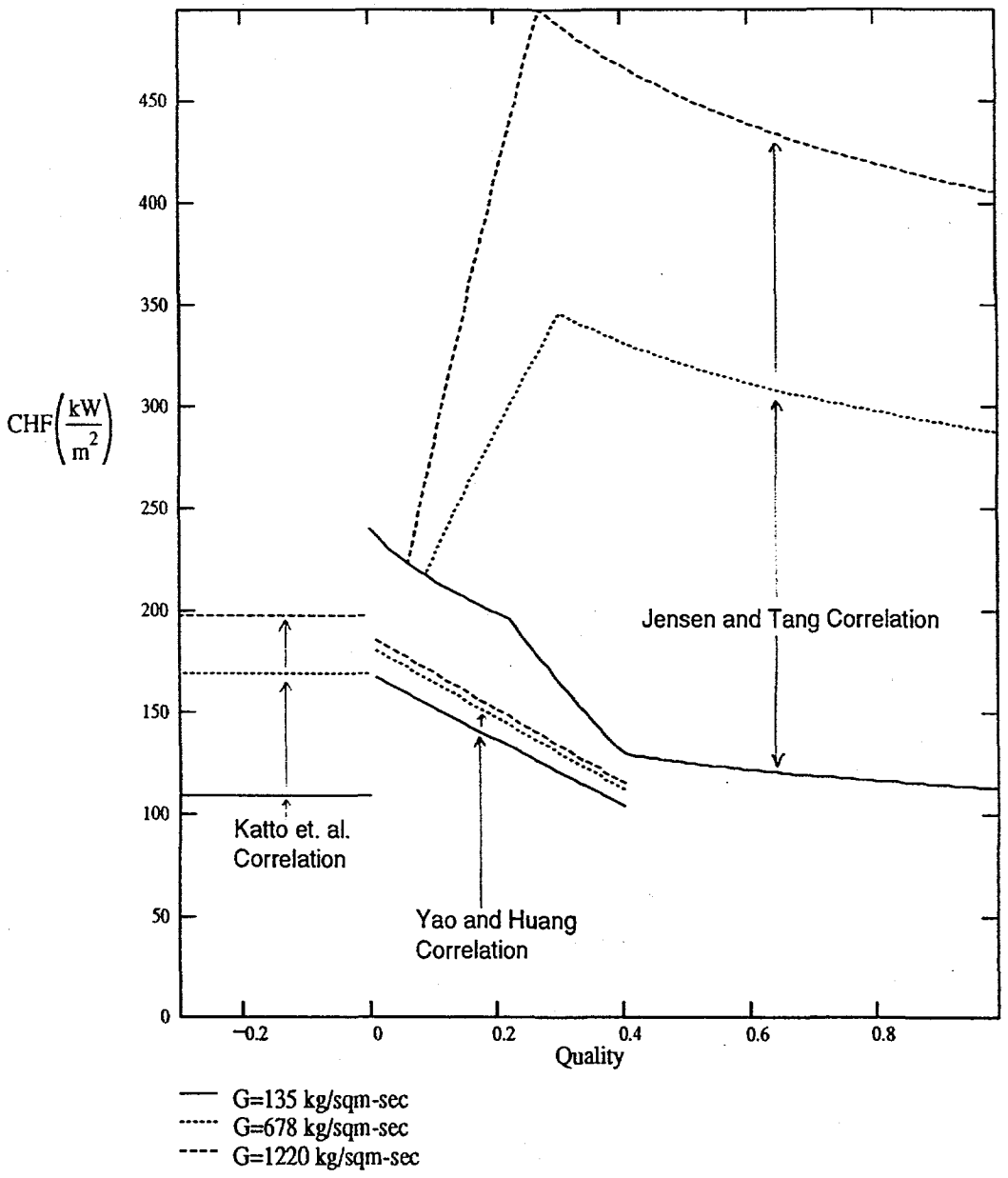

Figure 6: Predicted versus Measured CHF for G= 135 kg/m^{2}sec

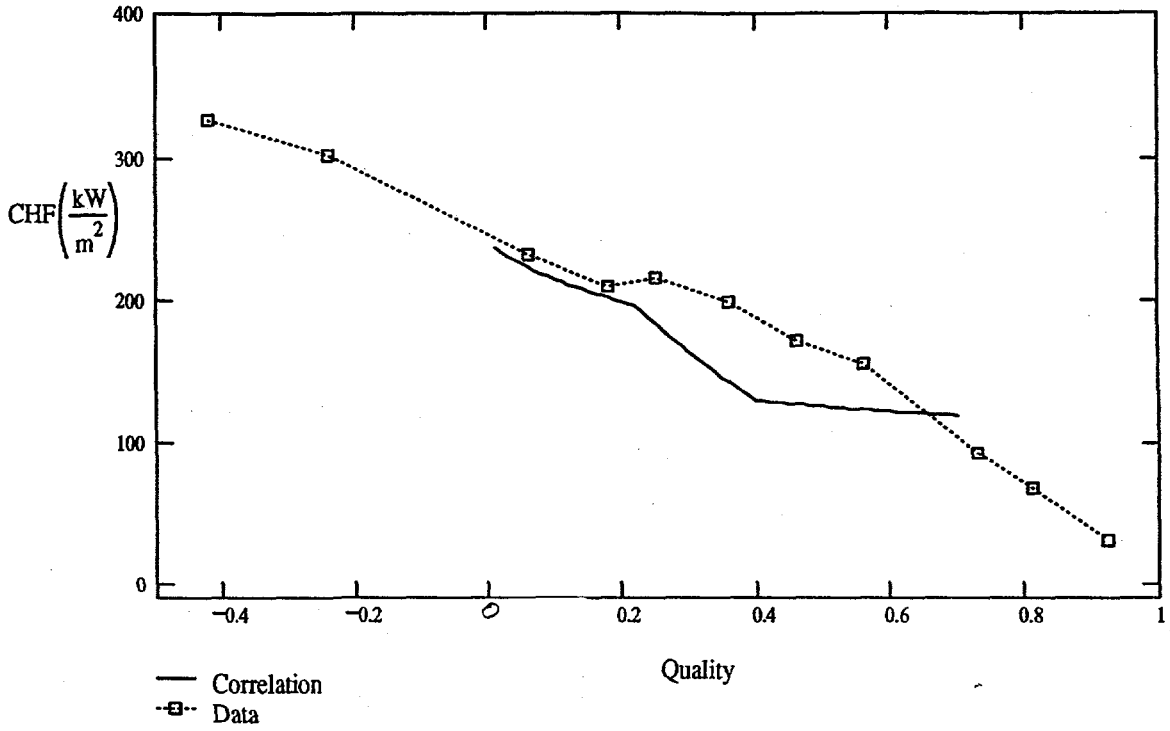

Figure 7: Predicted versus Measured CHF for G= 407 kg/m^{2}sec

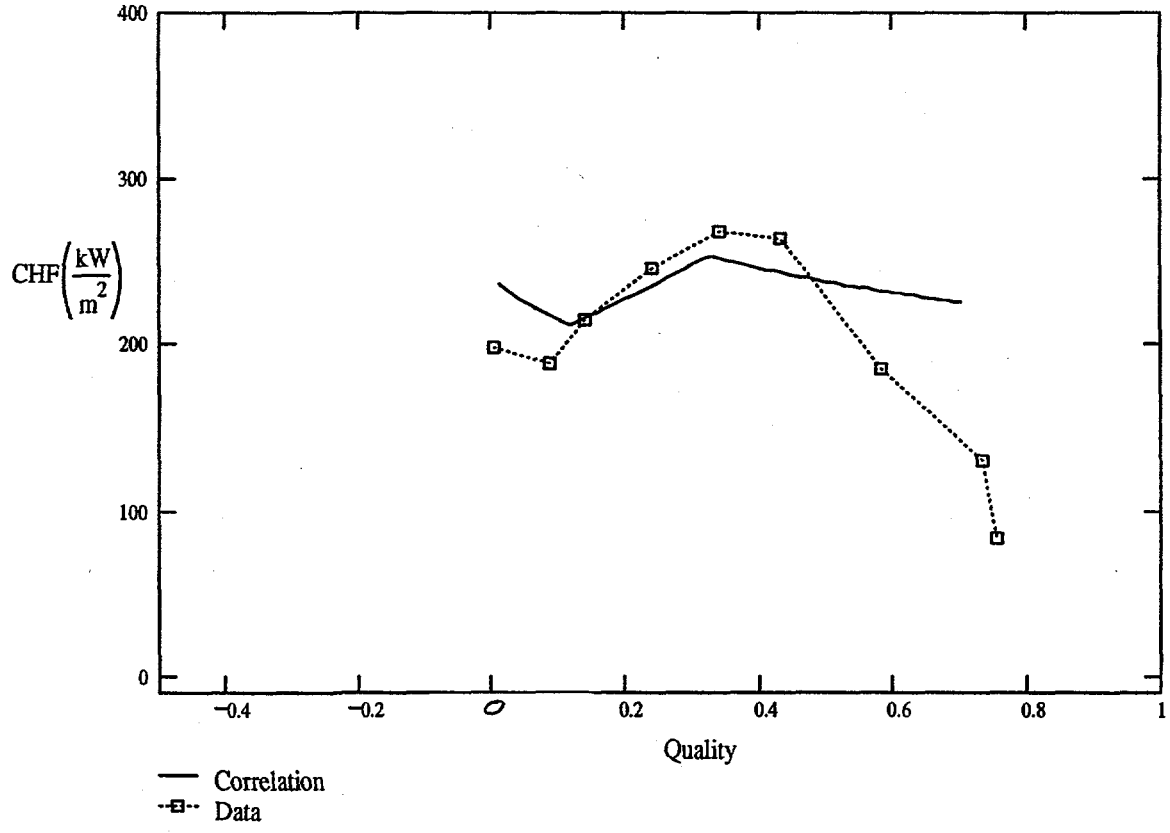

Figure 8: Predicted versus Measured CHF for G= 678 kg/m^{2}sec

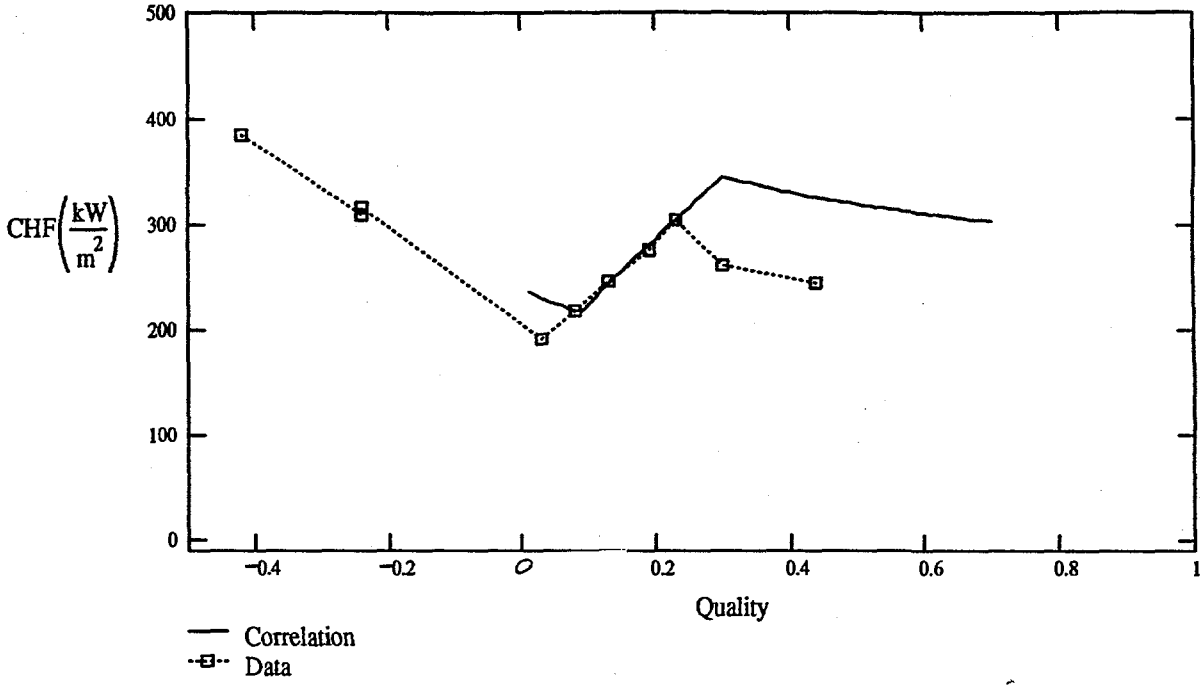

Figure 9: Predicted versus Measured CHF for G=950 kg/m^{2}sec

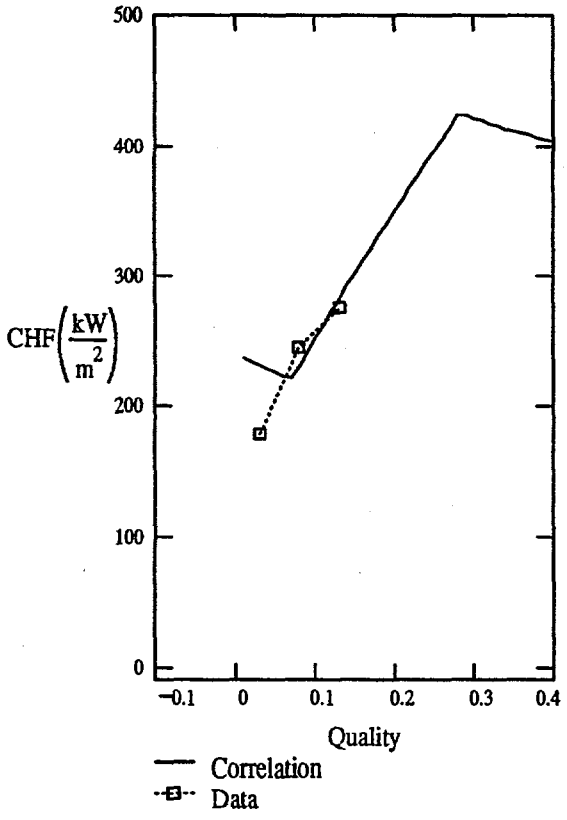

Figure 10: Predicted versus Measured CHF for G=1221 kg/m^{2}sec

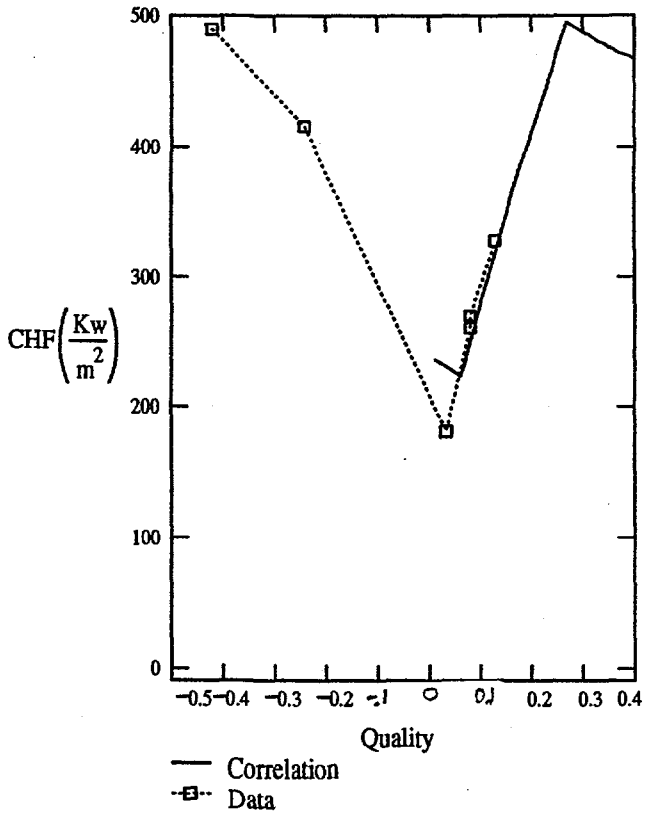

Figure 11: Predicted versus Measured CHF for Various Mass Fluxes

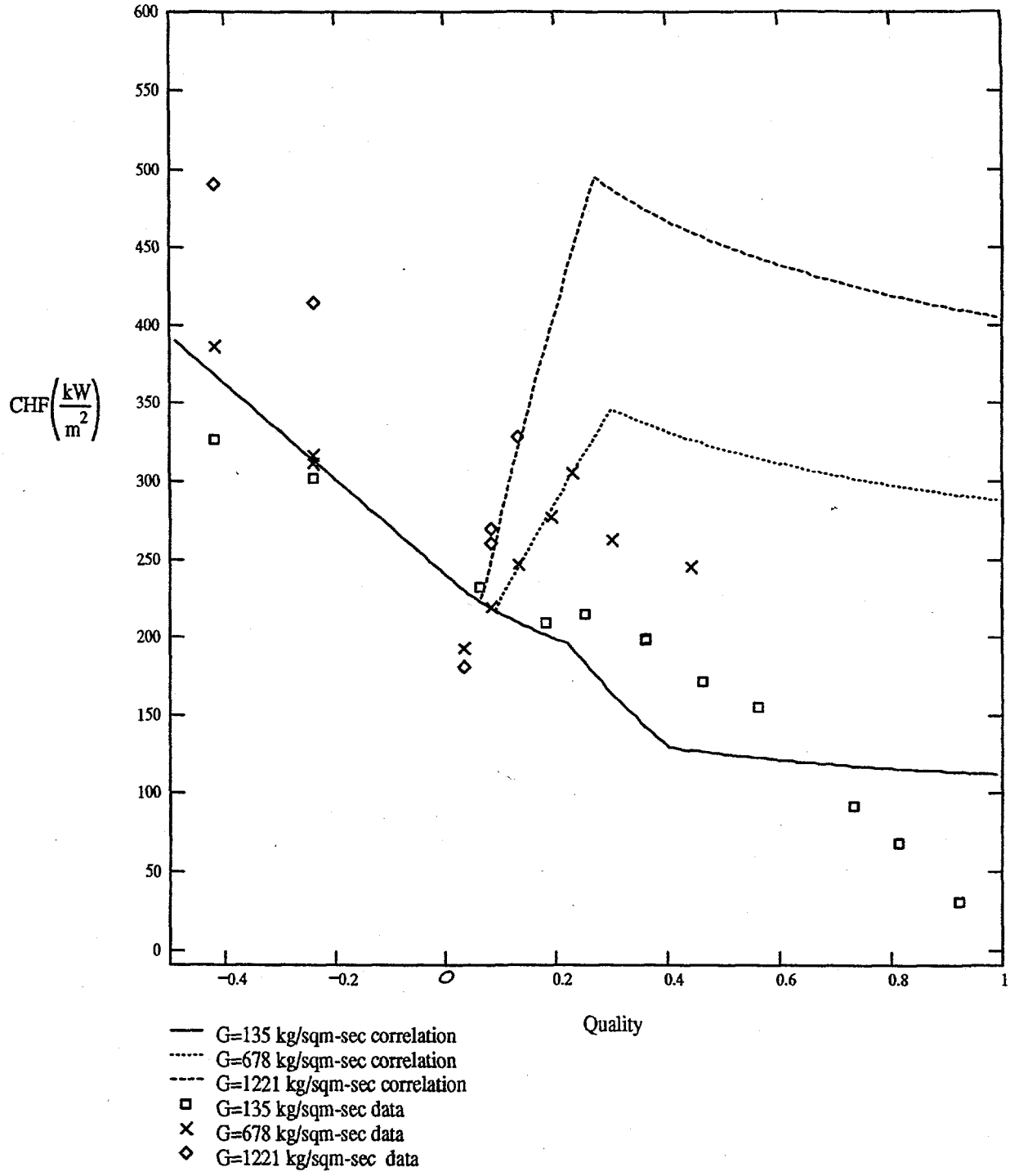

Appendix A
Sample Thermocouple Data and Strip Chart Recordings

Figure A.1

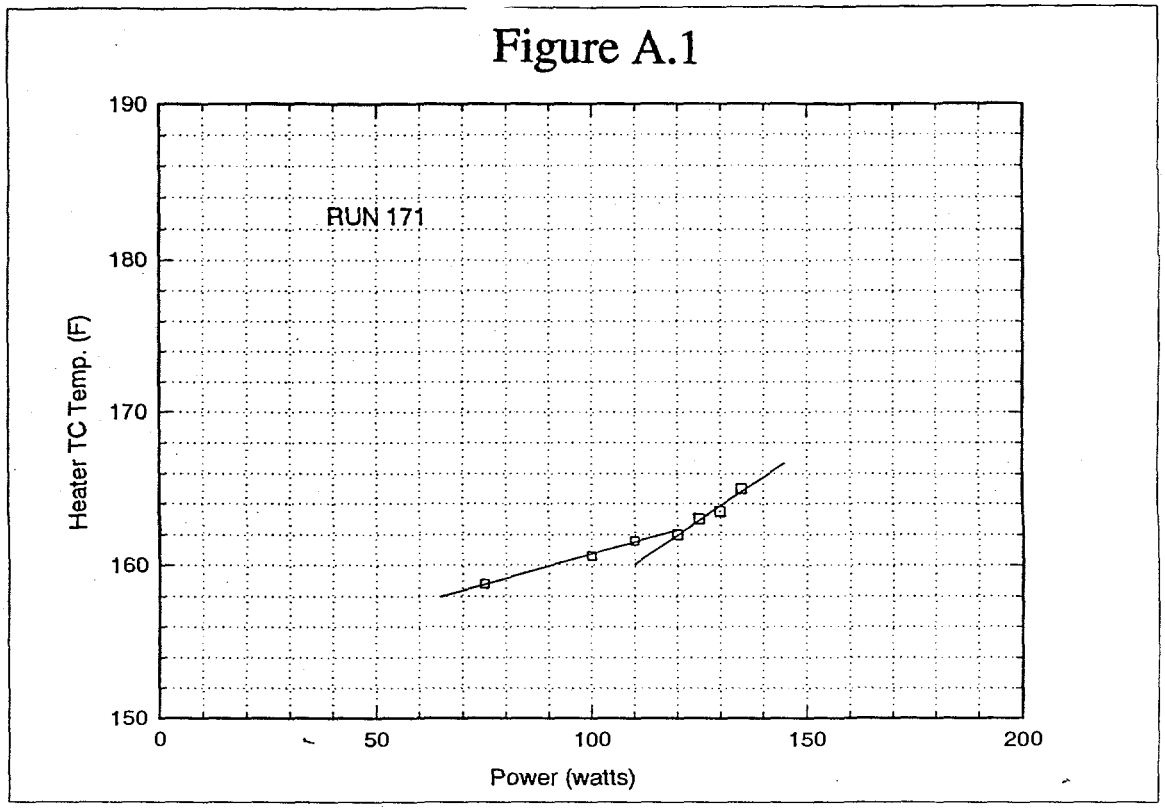

RUN 171

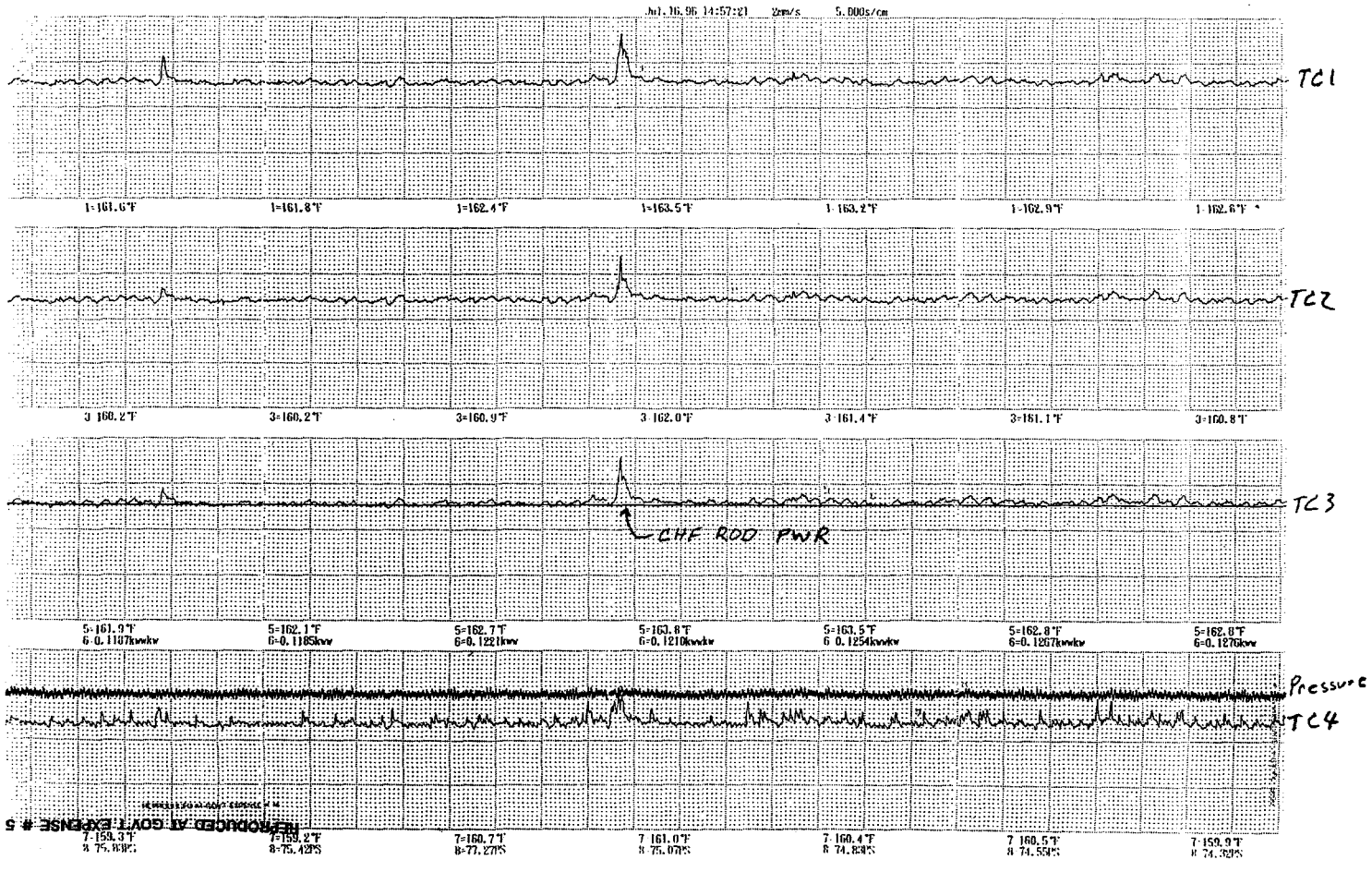

Figure A.2

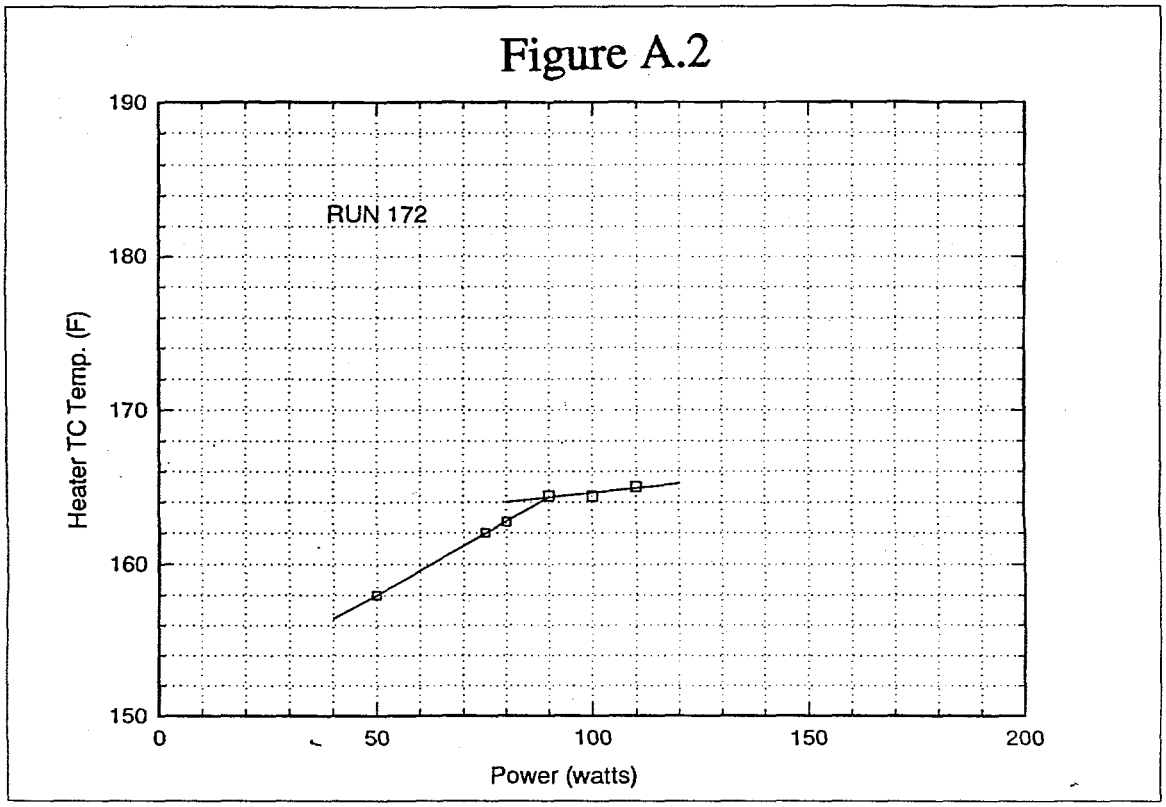

RUN 172

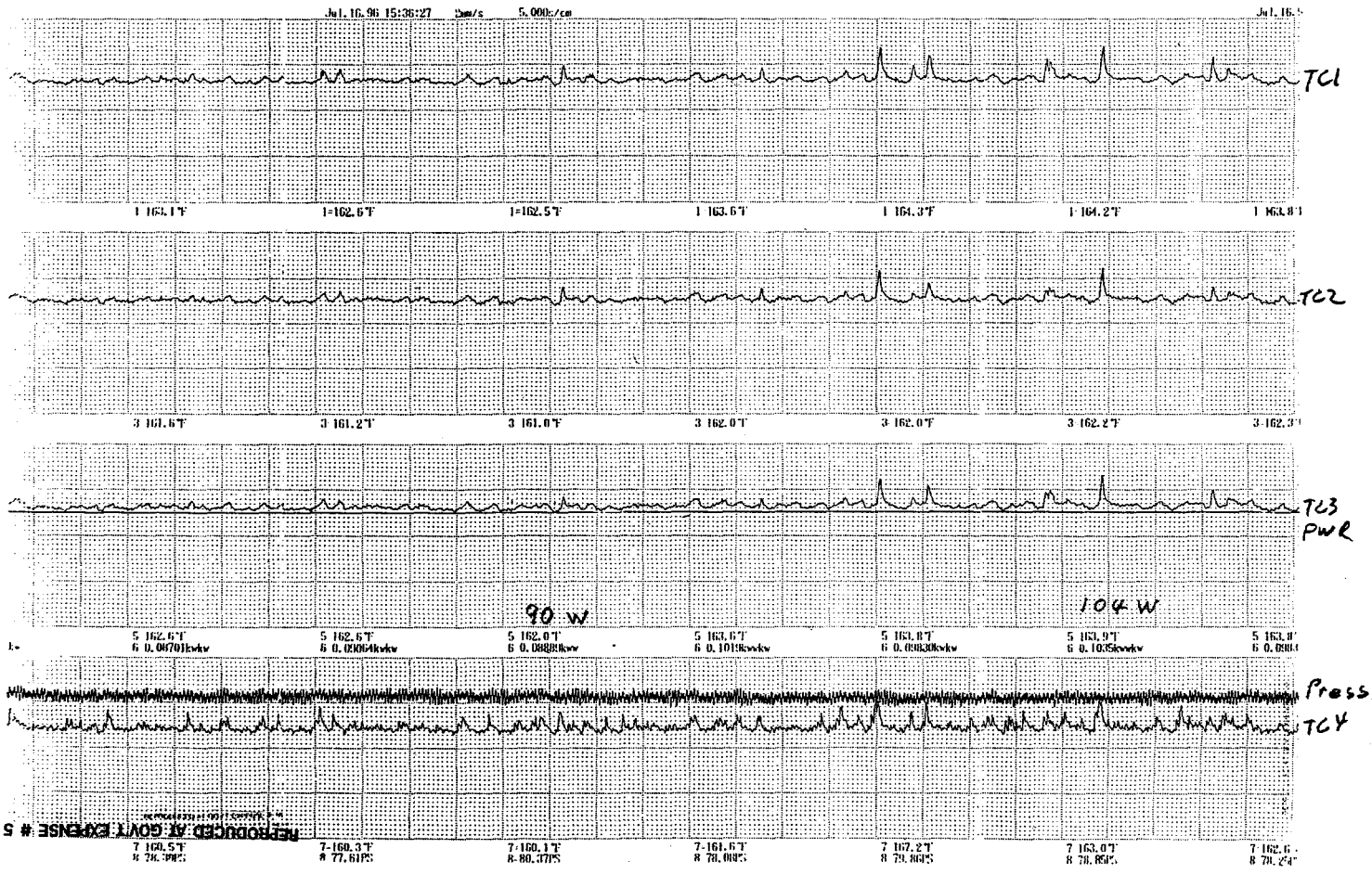

Figure A.3

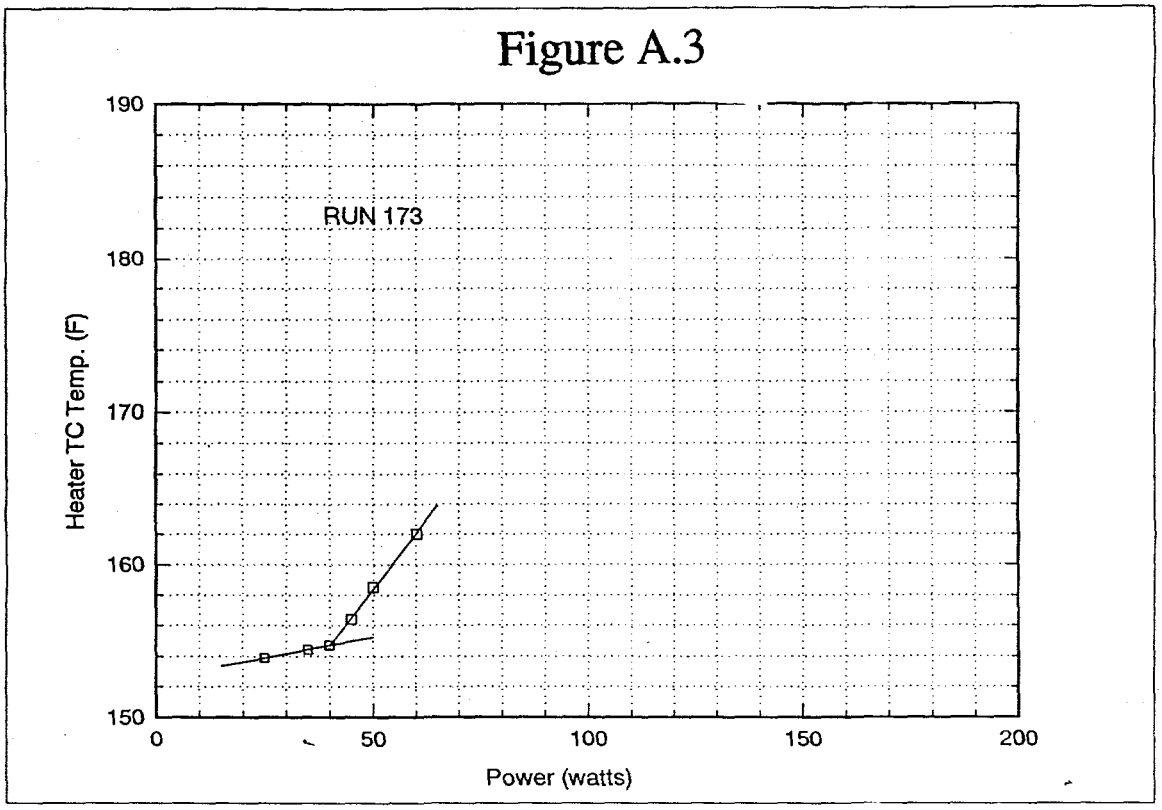
RUN 173
Heater TC Temp. (F)
190
180
170
160
150
0
50
100
150
200
Power (watts)

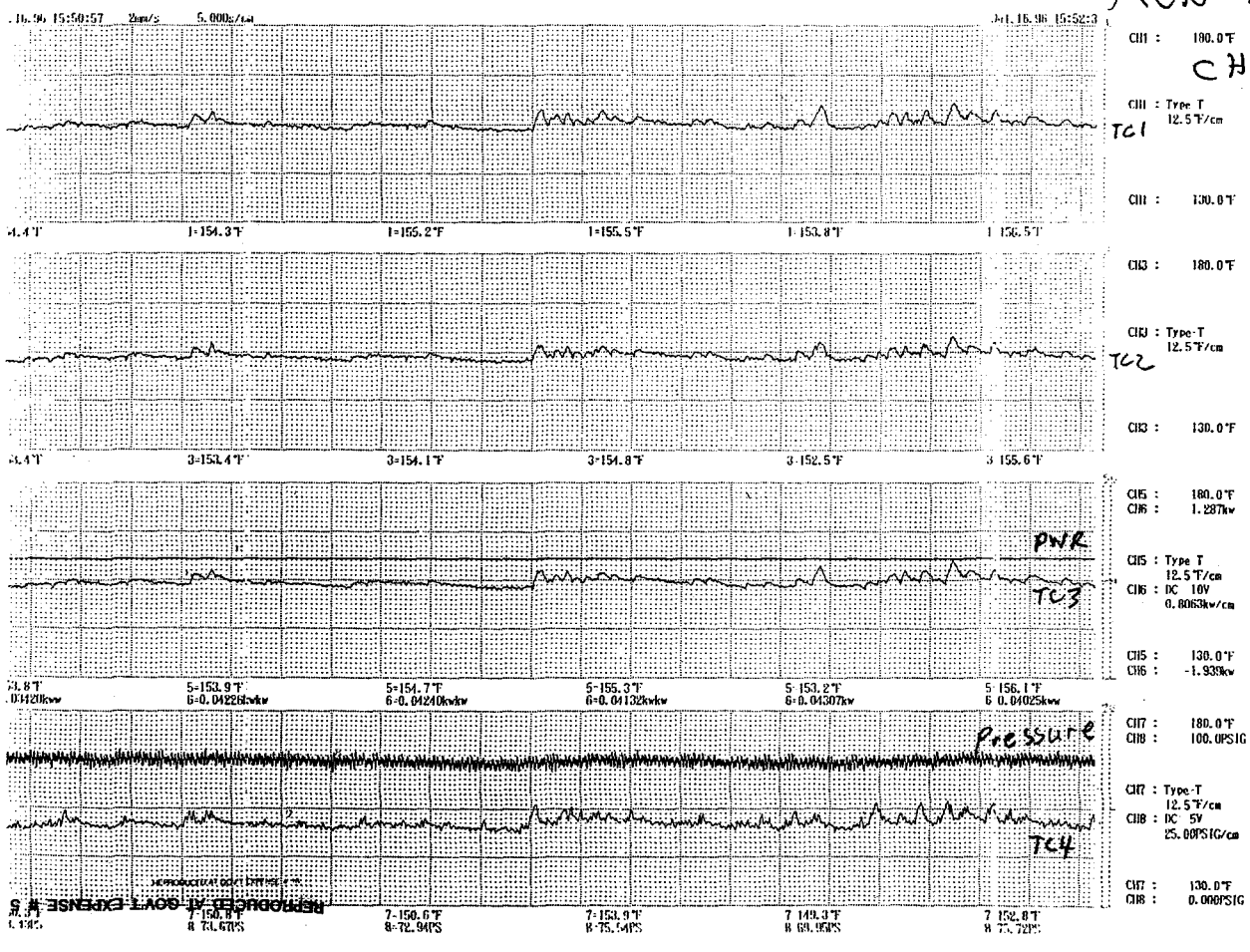
RUN 173
CHF ~ 42
CH1 : 180.0°F
CH1 : Type T
12.5°F/cm
TC1
CH1 : 130.0°F
CH3 : 180.0°F
CH3 : Type-T
12.5°F/cm
TC2
CH3 : 130.0°F
CH5 : 180.0°F
CH6 : 1.287kw
PWR
CH5 : Type T
12.5°F/cm
CH6 : DC 10V
0.8063kw/cm
TC3
CH5 : 130.0°F
CH6 : -1.939kw
CH7 : 180.0°F
CH8 : 100.0PSIG
Pressure
CH7 : Type-T
12.5°F/cm
CH8 : DC 5V
25.00PSIG/cm
TC4
CH7 : 130.0°F
CH8 : 0.000PSIG

Figure A.4

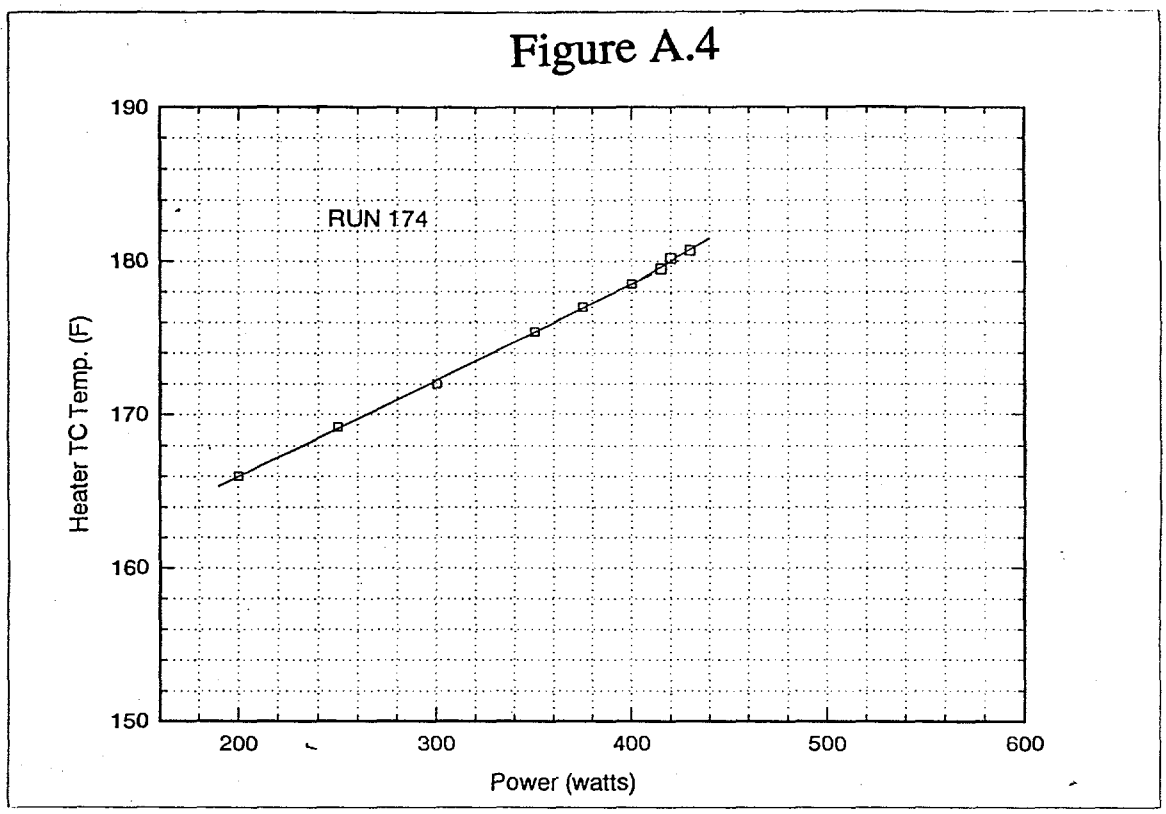

RUN 174

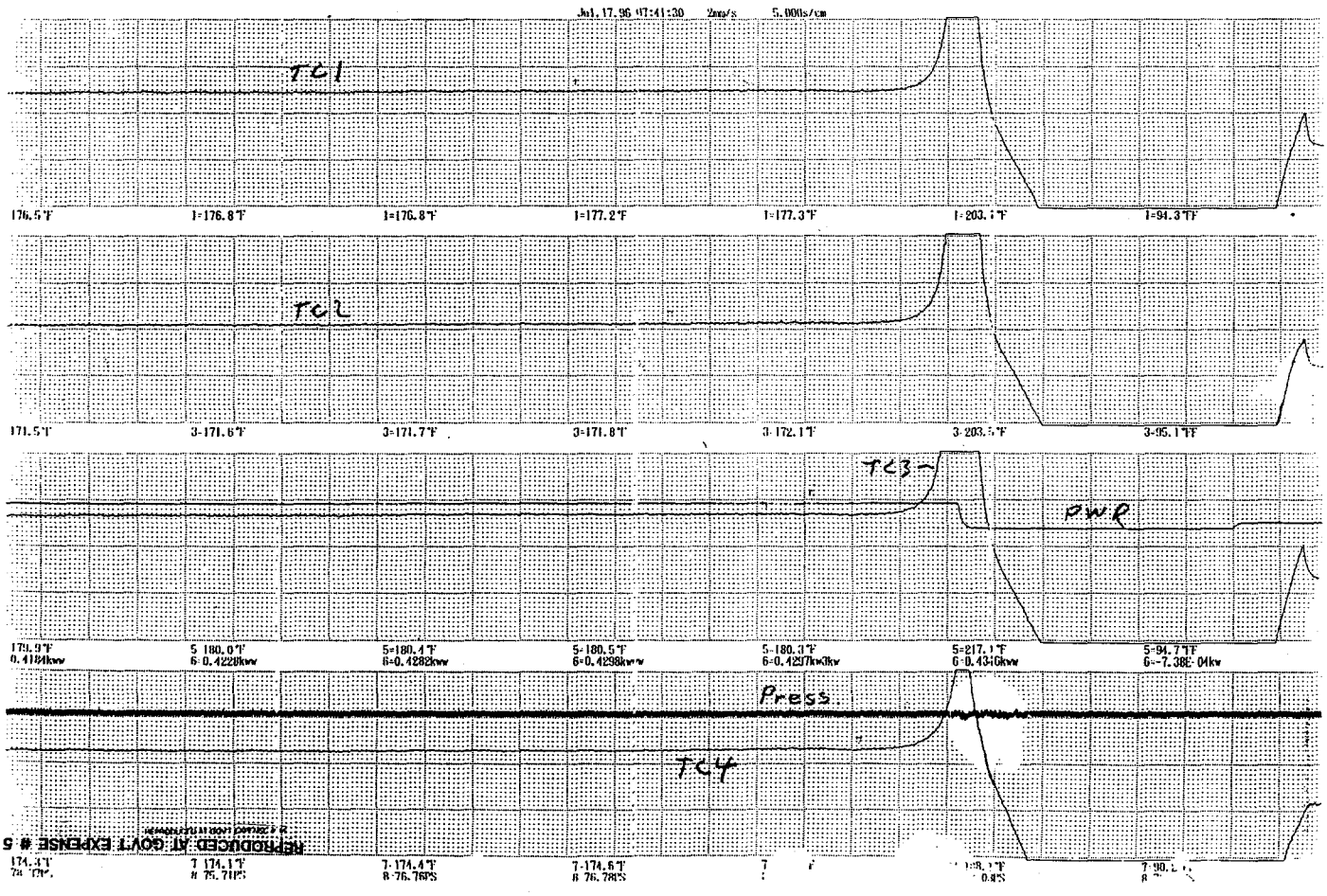

Figure A.5

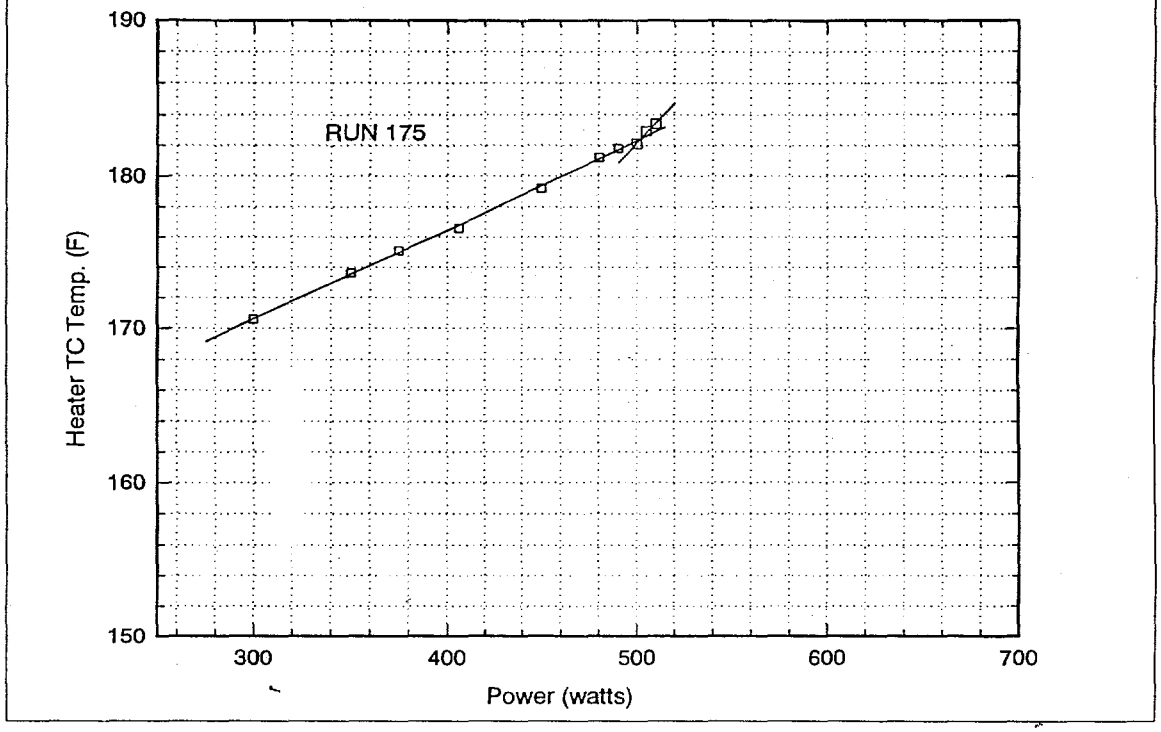

RUN 175

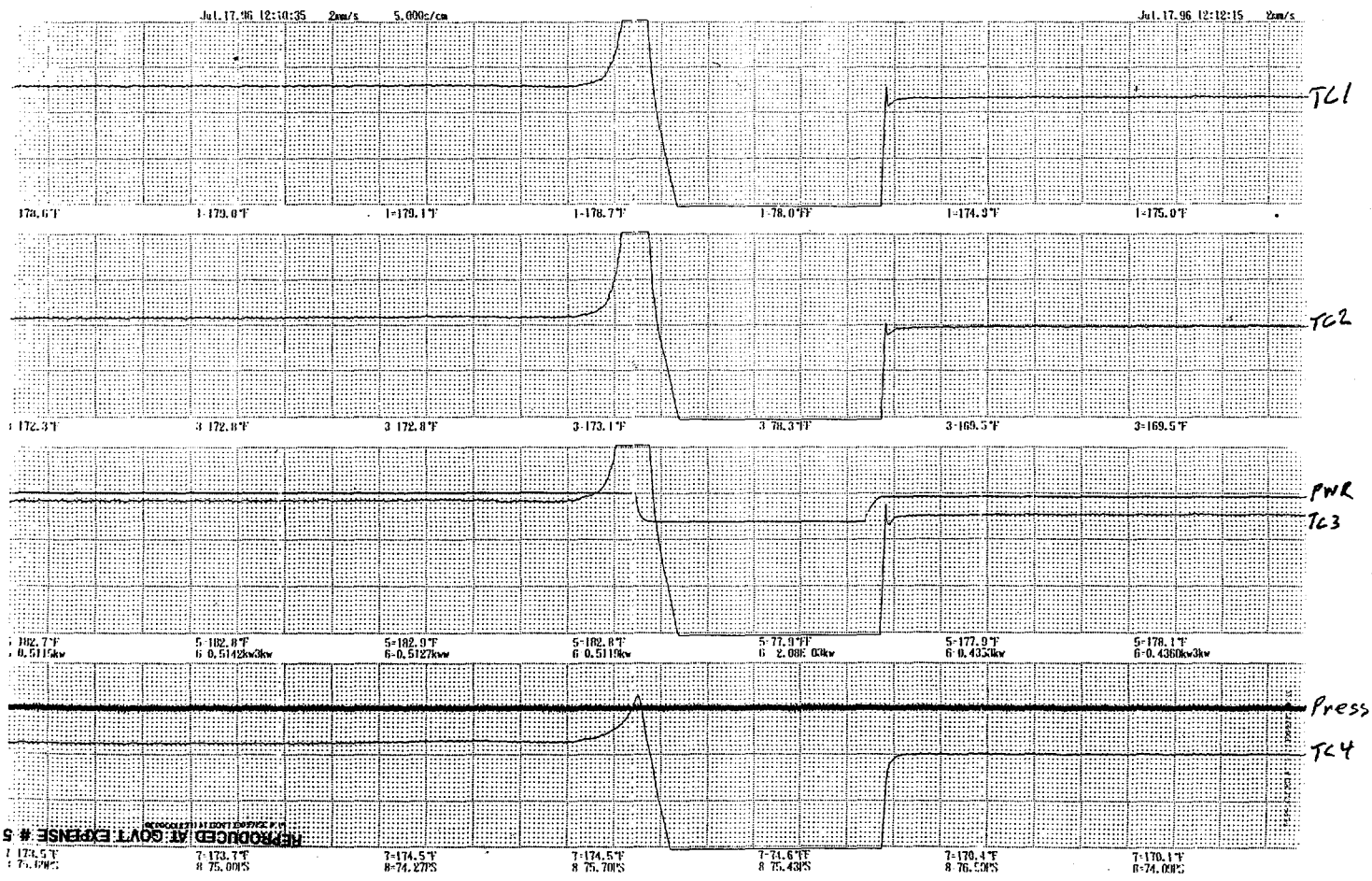

Figure A.6

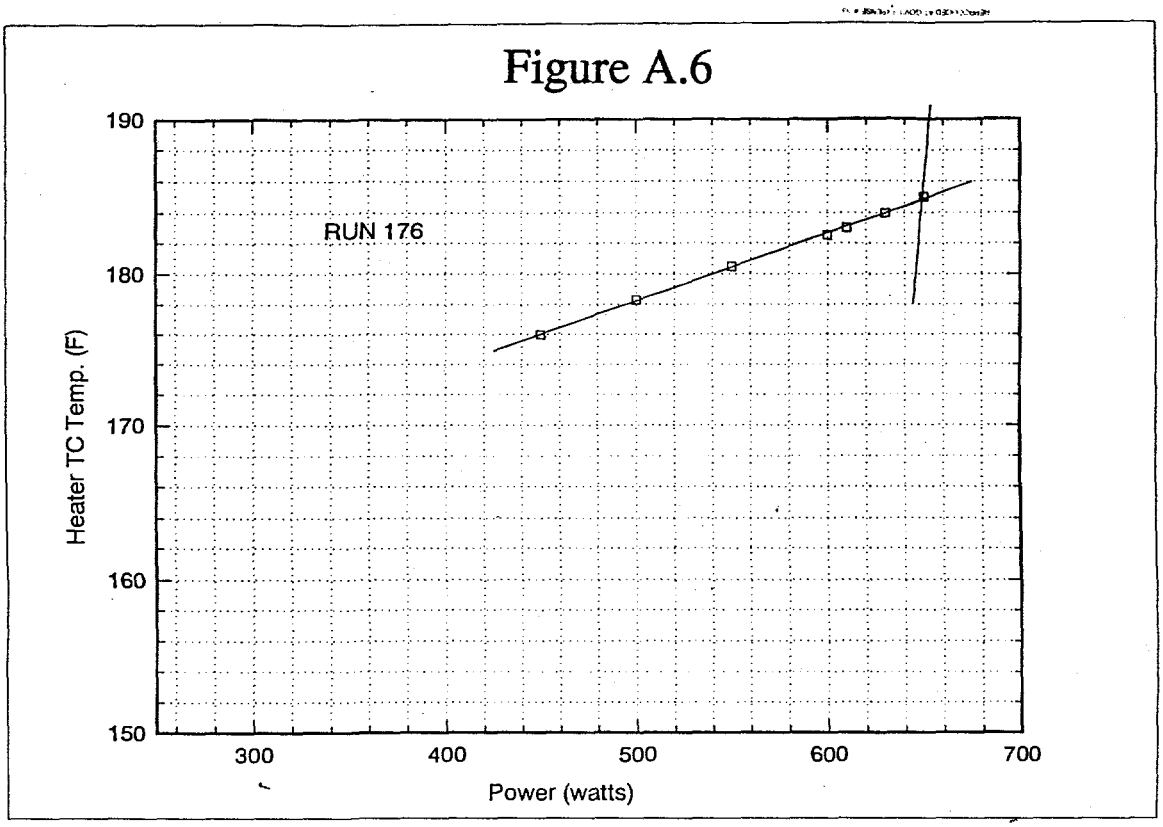

RUN 176

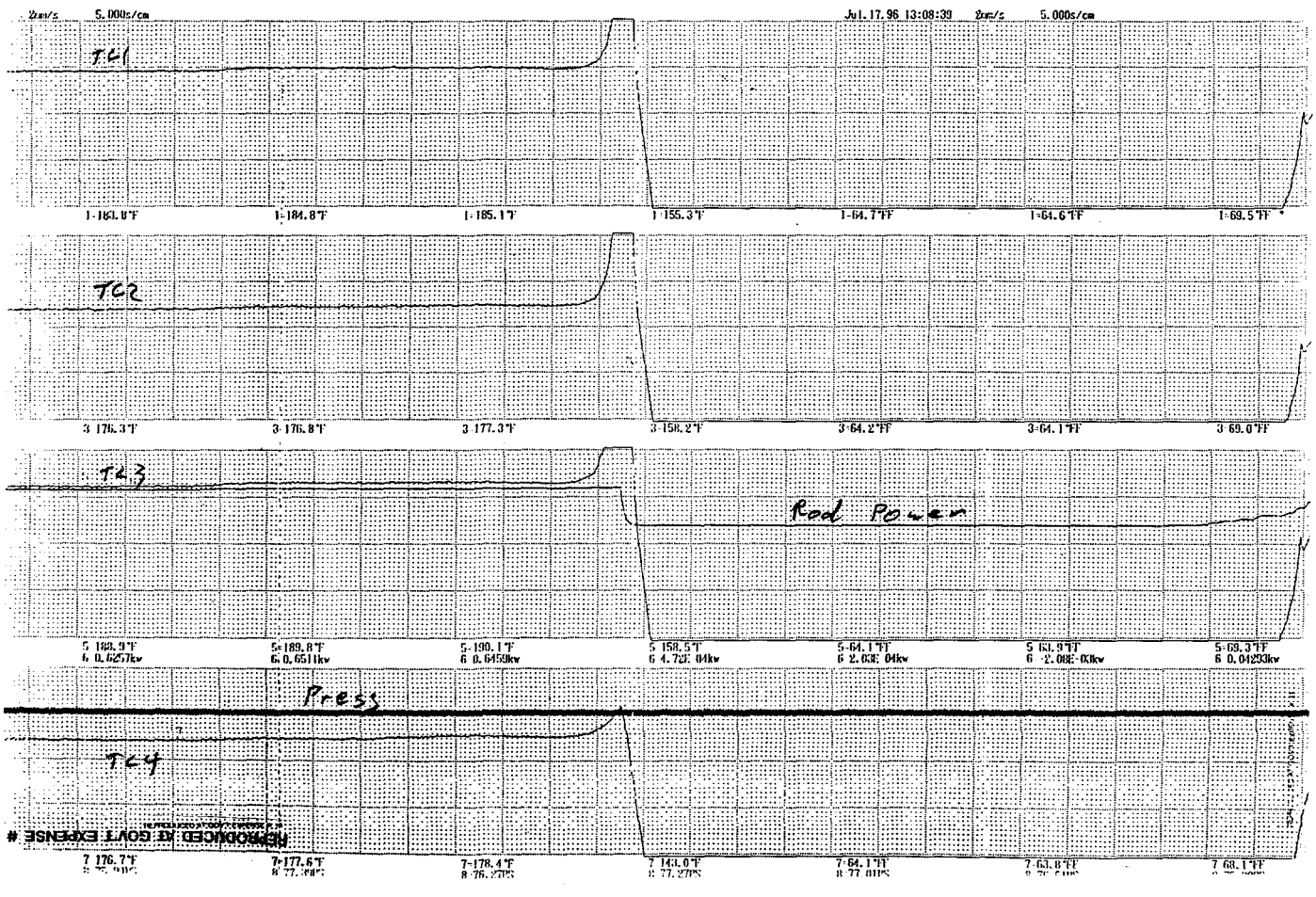

Figure A.7

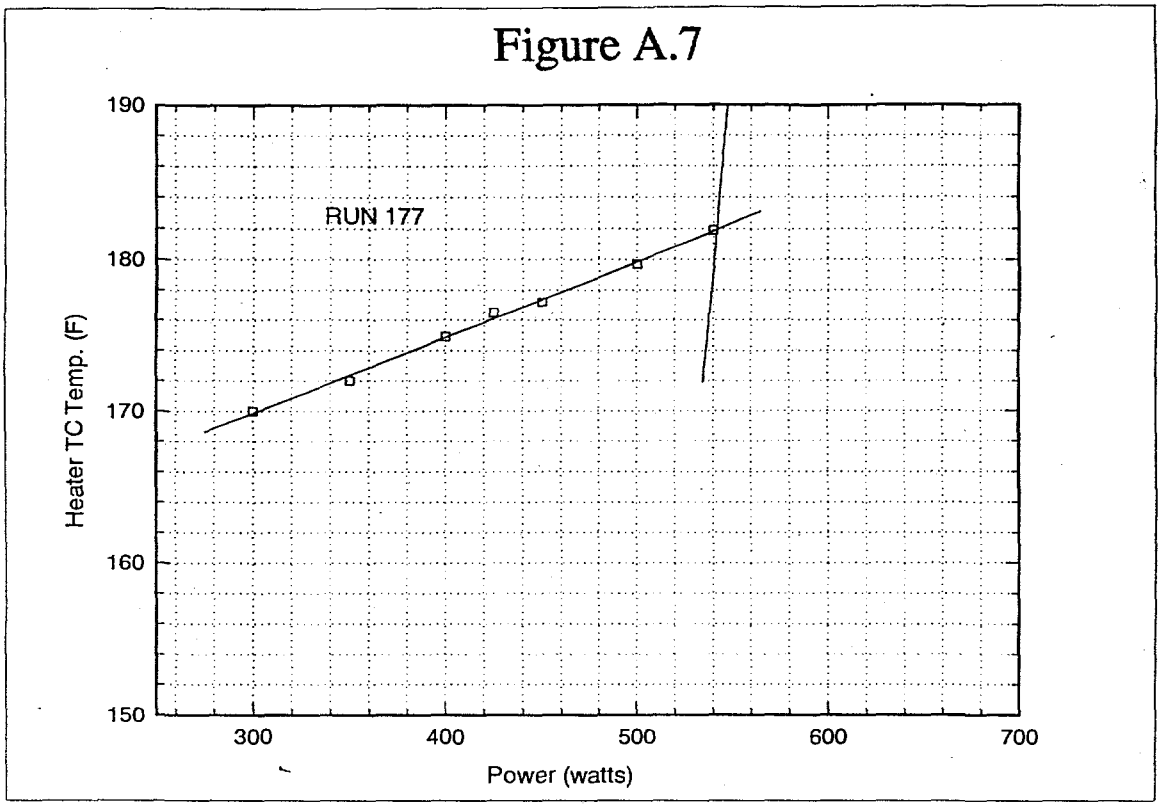

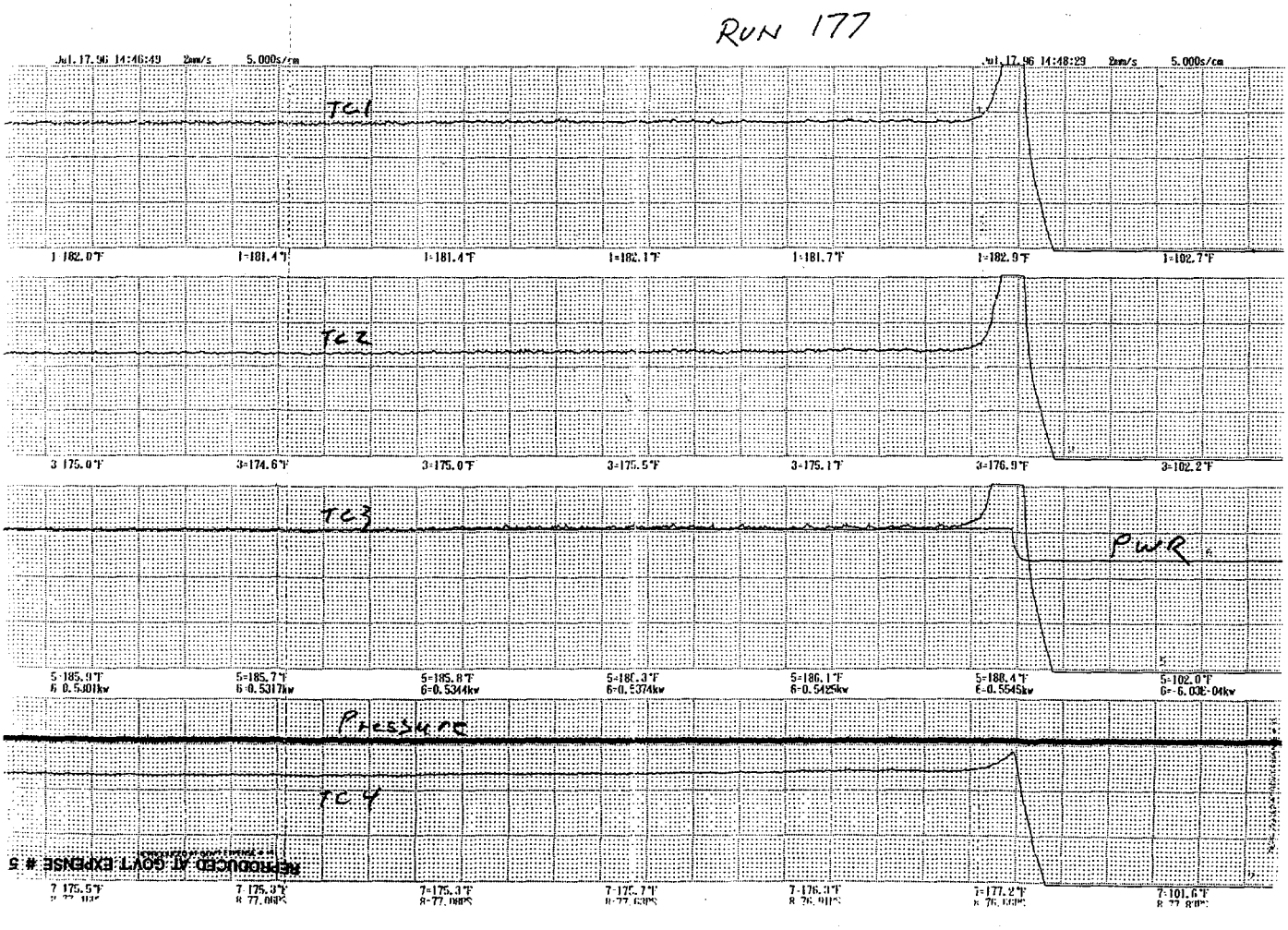

Figure A.8

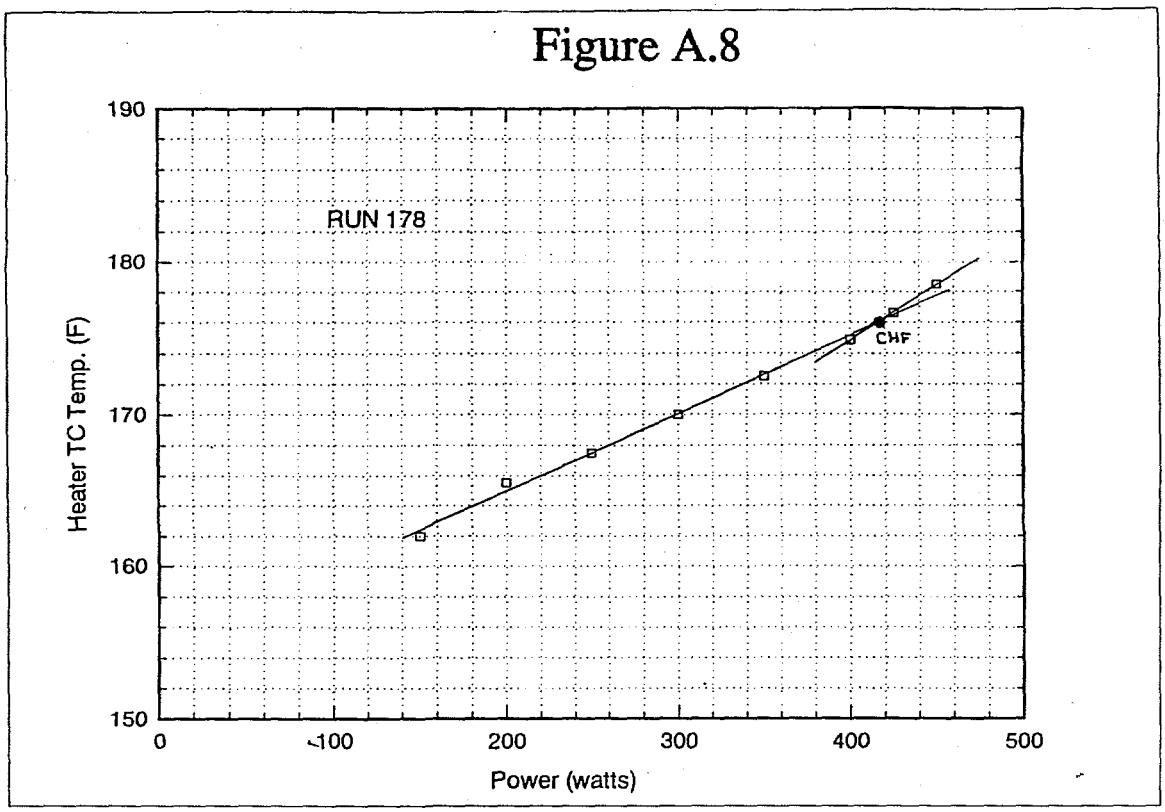

RUN 178

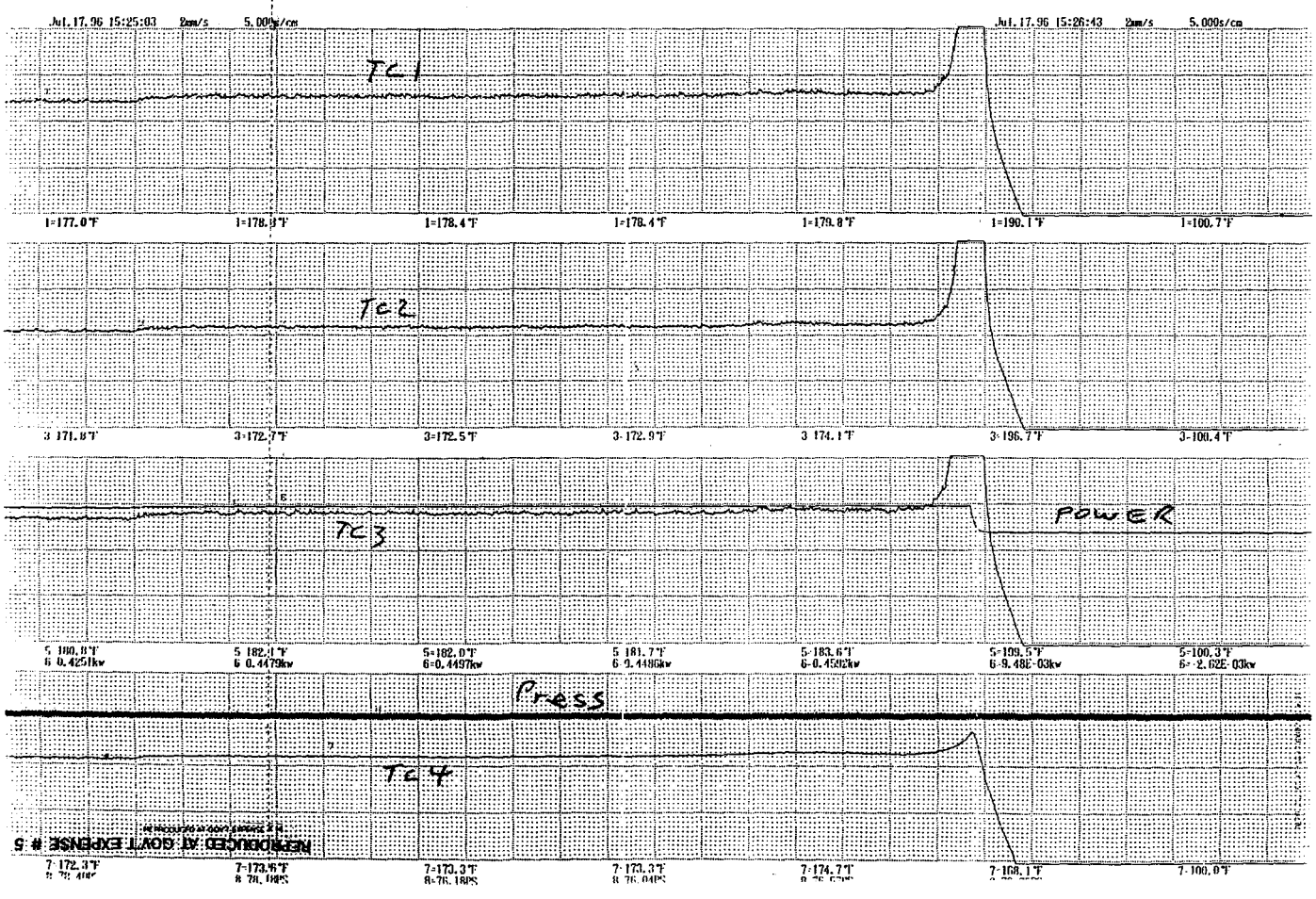

Figure A.9

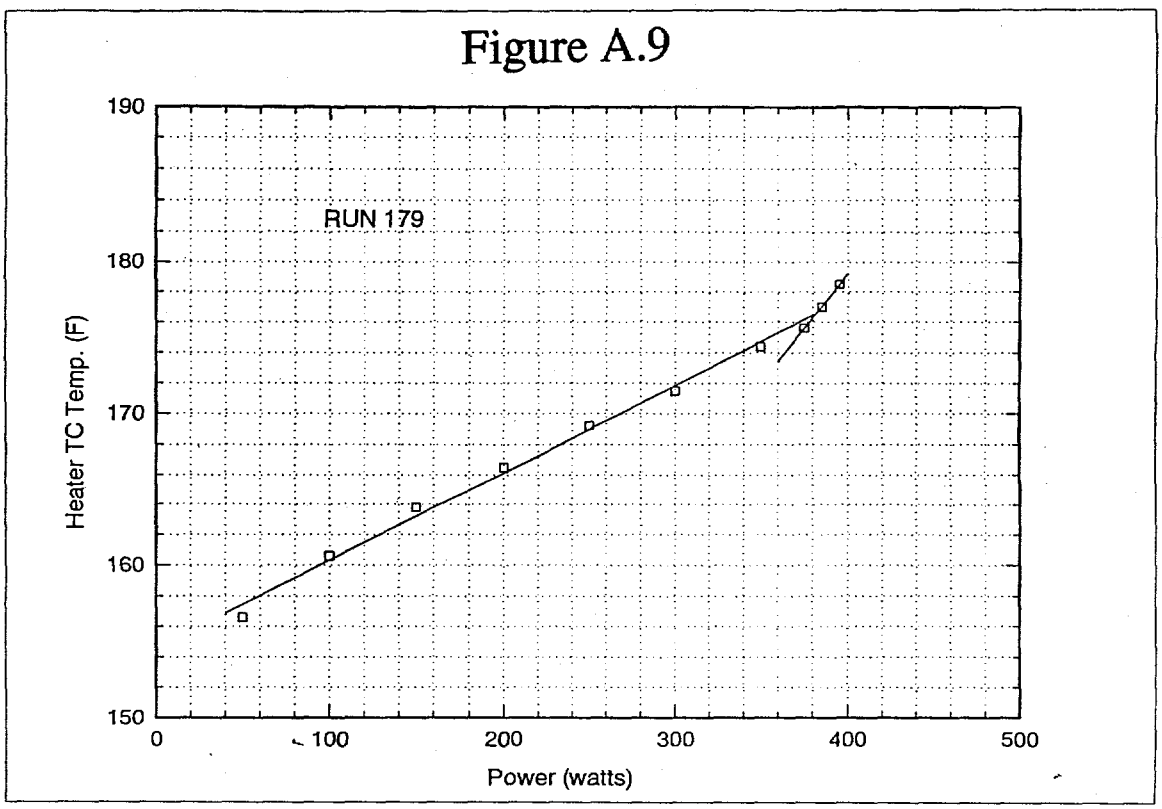

RUN 179

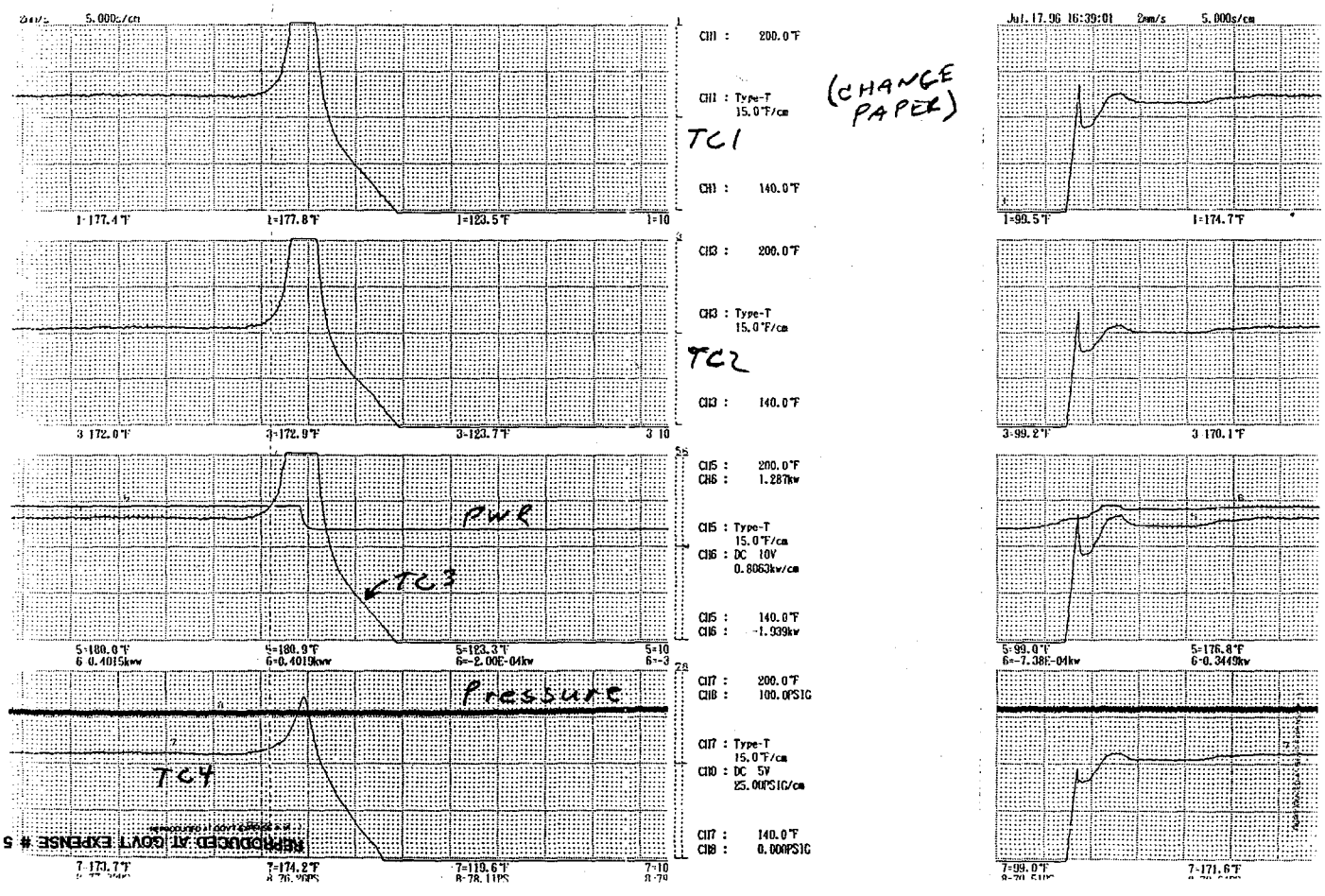

Figure A.10

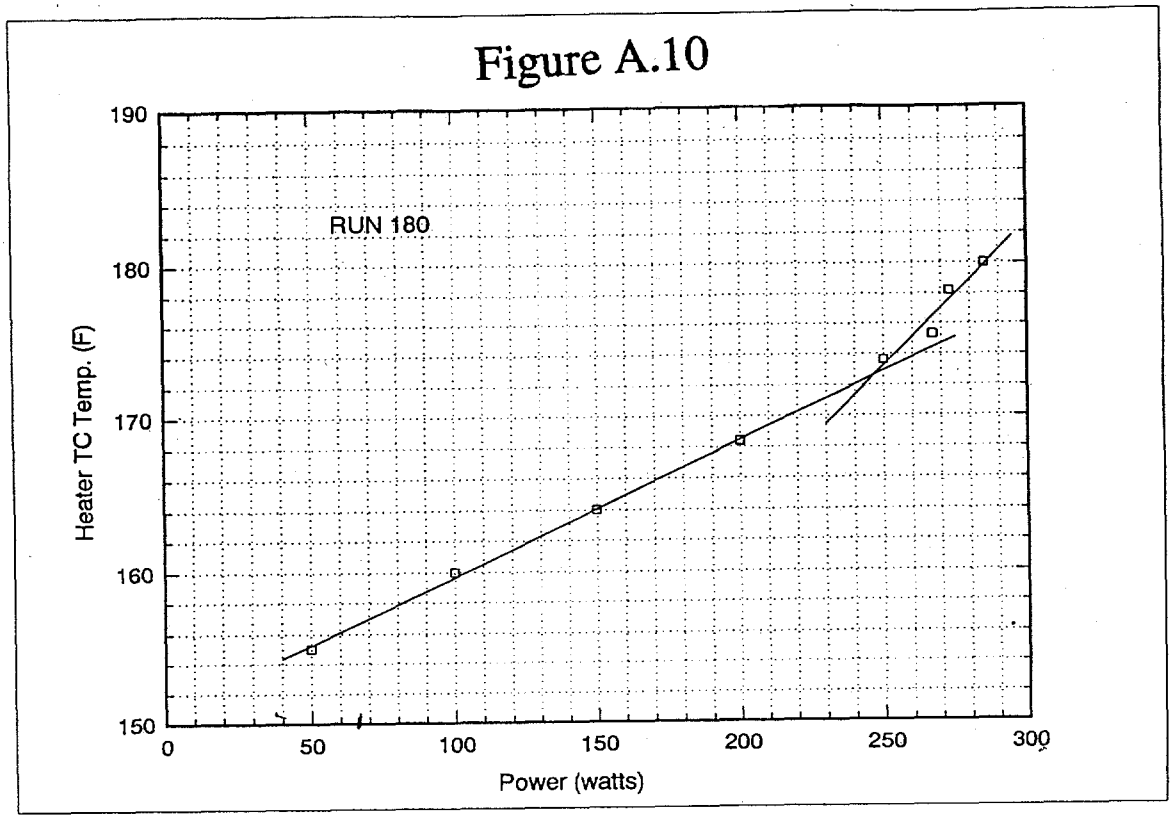

RUN 180

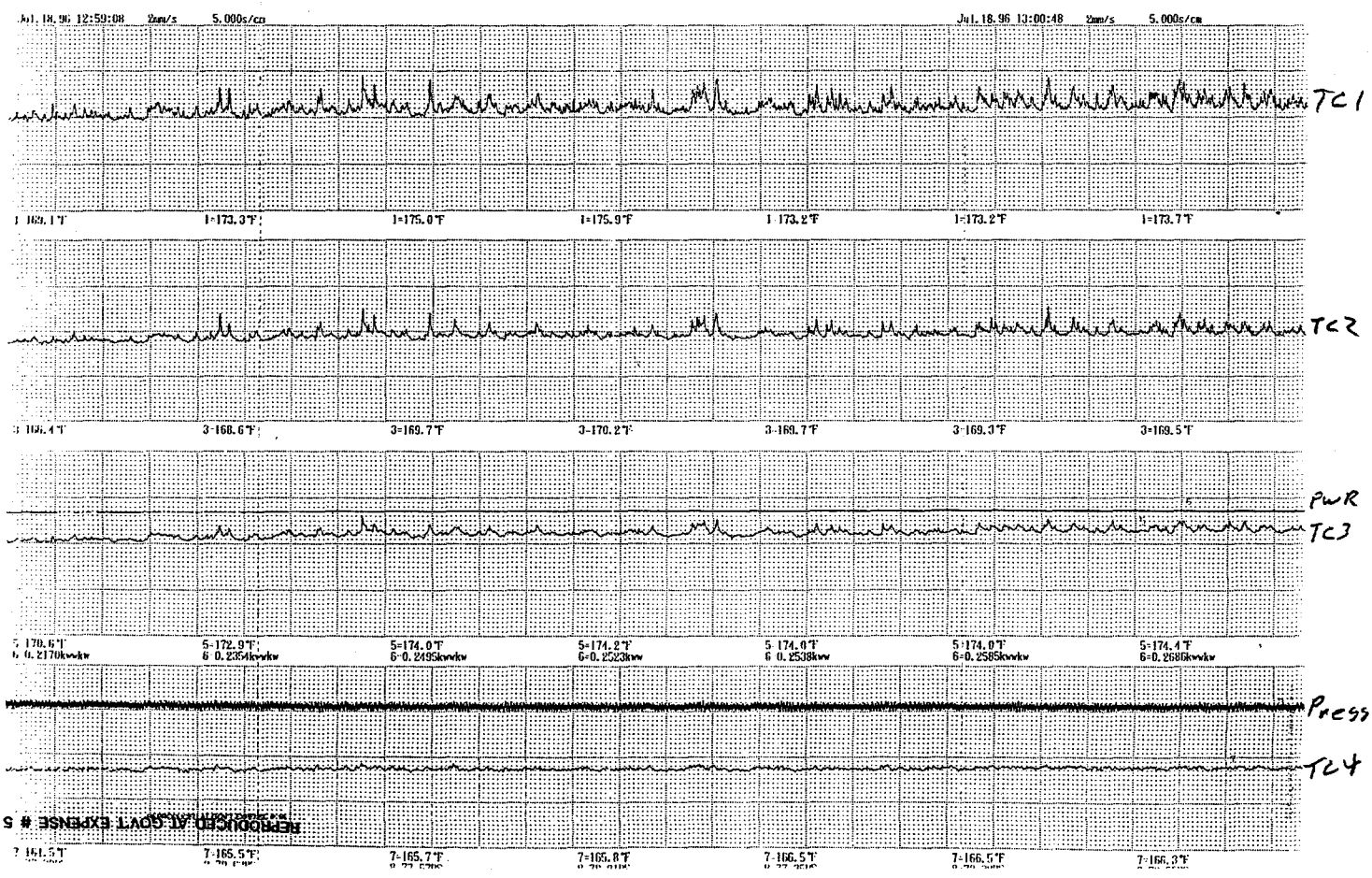

Figure A.11

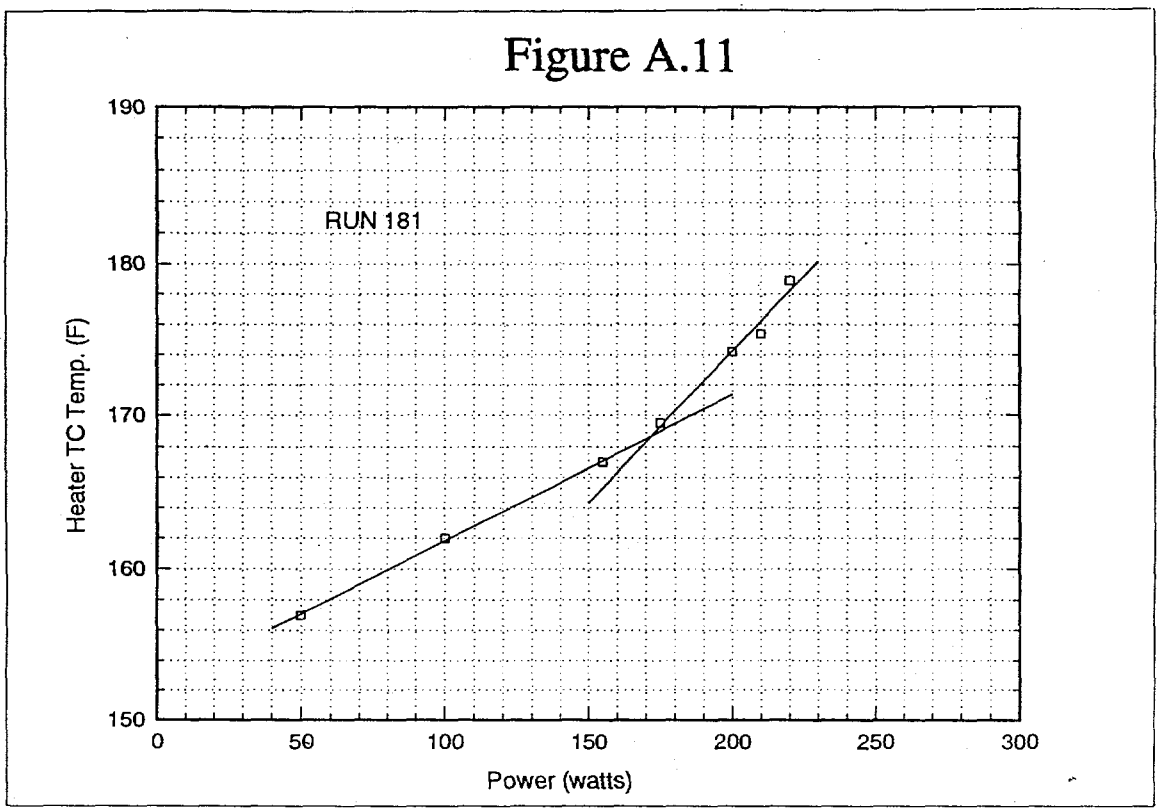

RUN 181

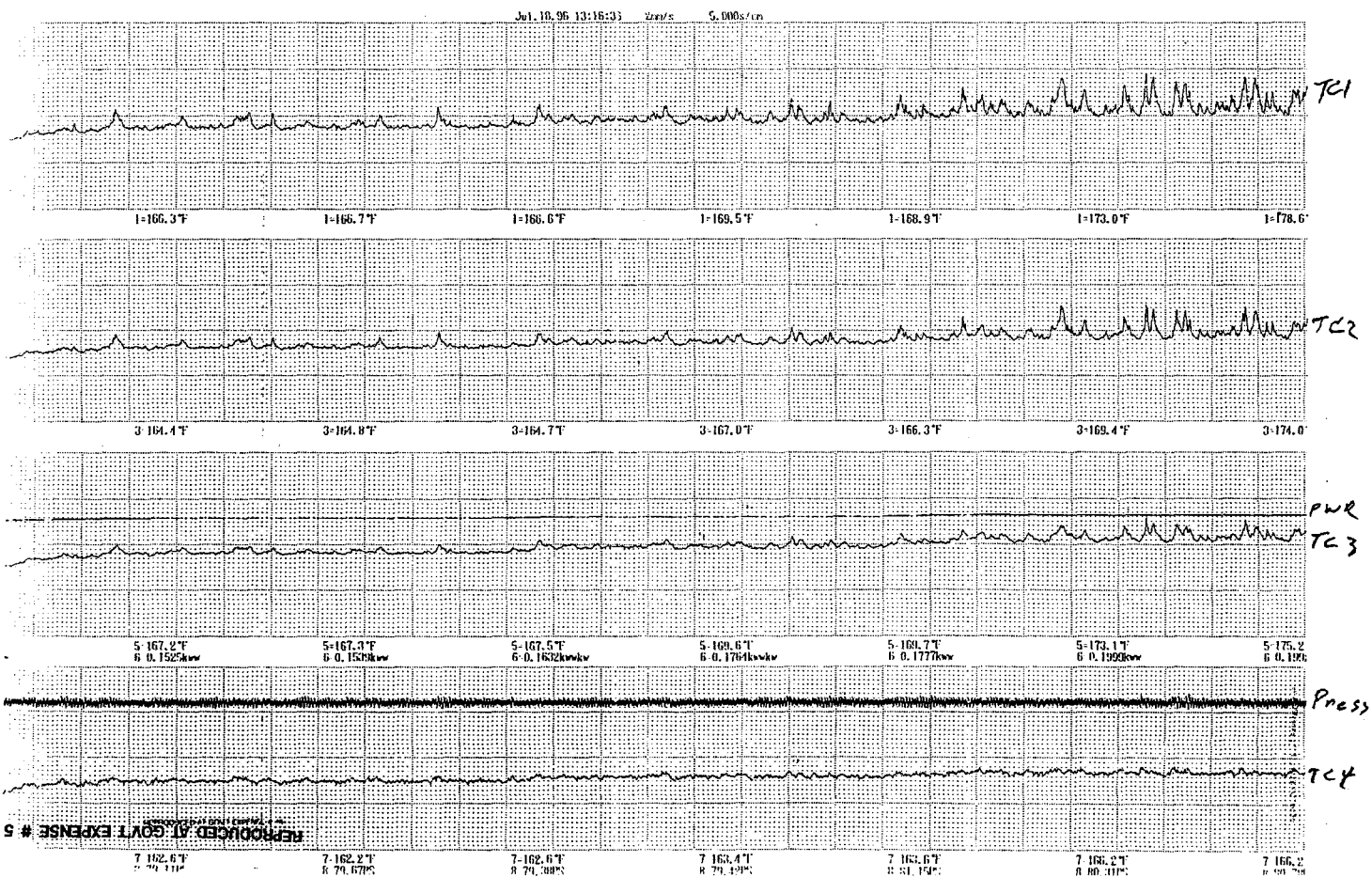

Figure A.12

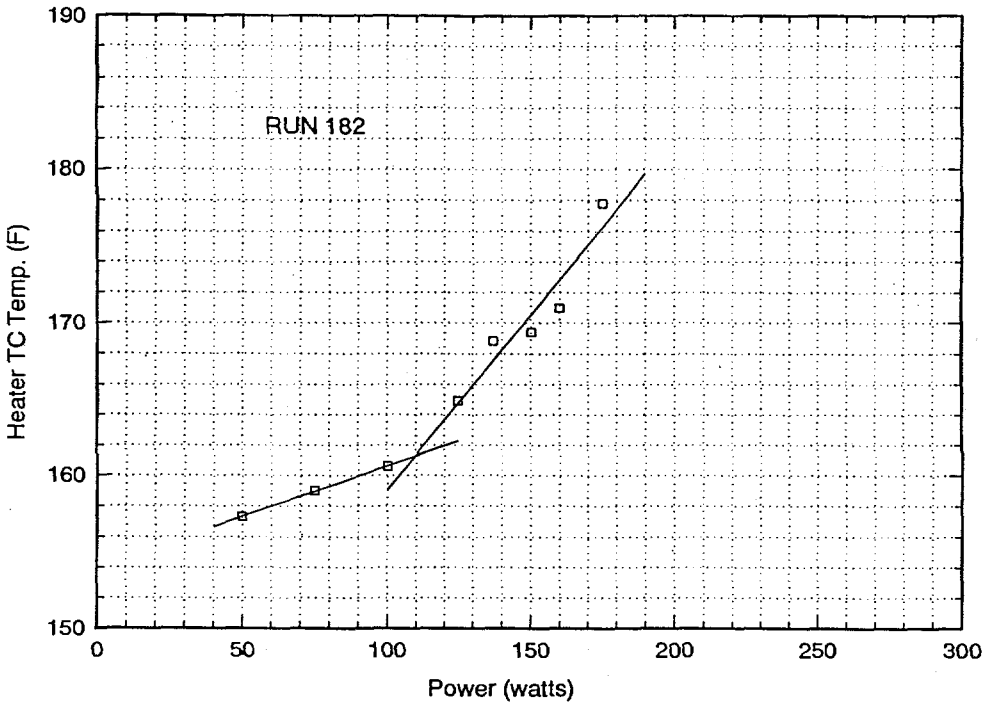
RUN 182
Heater TC Temp. (F)
Power (watts)
190
180
170
160
150
0
50
100
150
200
250
300

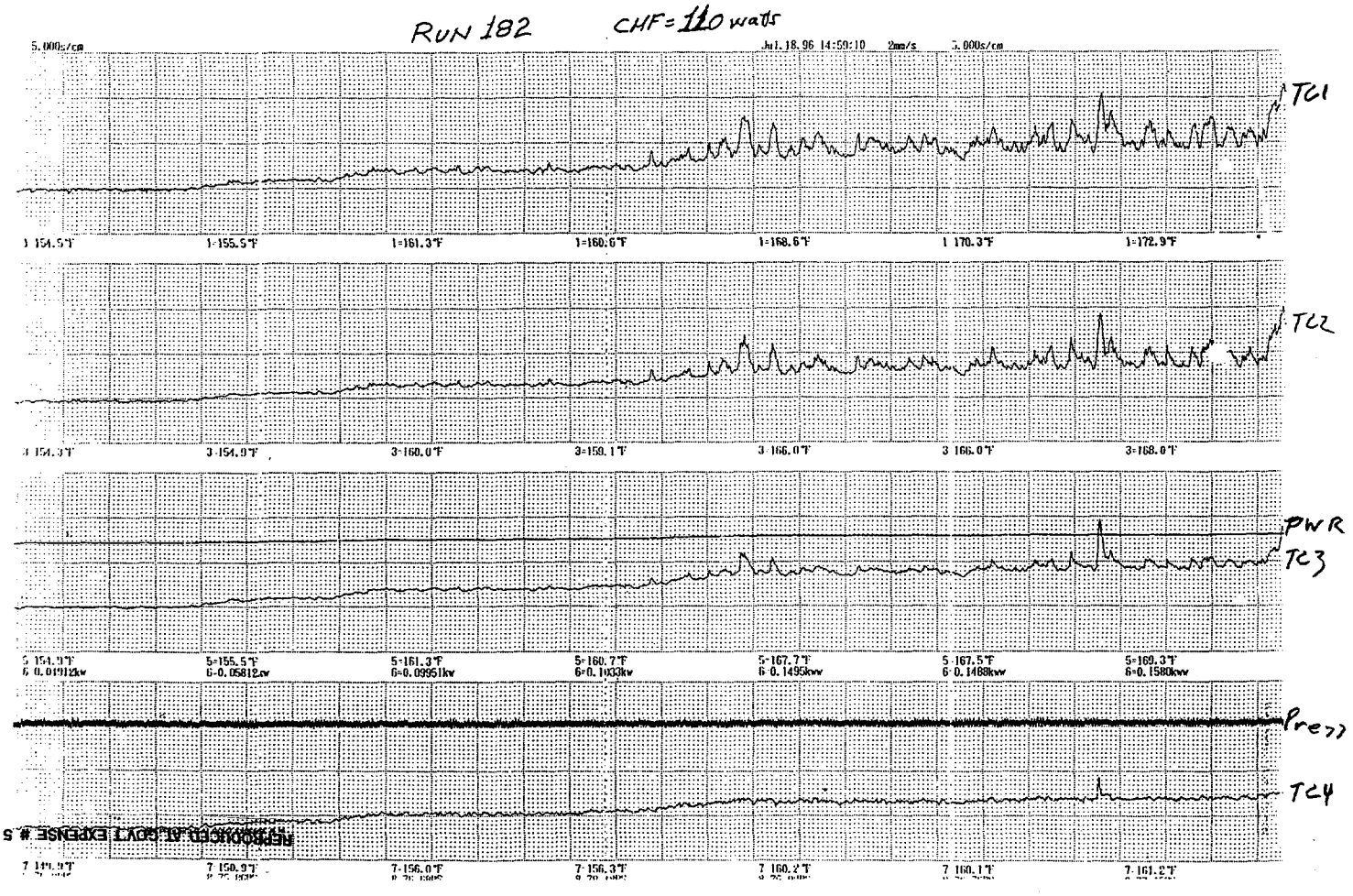
RUN 182
CHF = 110 watts
TC1
TC2
PWR
TC3
Pres
TC4